



WPI

Design of a Patellofemoral Unloader Knee Brace

A Major Qualifying Project
Submitted to the Faculty of
WORCESTER POLYTECHNIC INSTITUTE
In partial fulfillment for the
Degree of Bachelor of Science

Submitted by:

Ramona Bago, Michael DiStefano, Jennifer Gomes, Caitlin Kyaw, Megan Pinette

May 13, 2020

Professor Sakthikumar Ambady, Ph.D., Advisor
Department of Biomedical Engineering

Professor Ahmet Can Sabuncu, Ph.D., Advisor
Department of Mechanical Engineering

Robert J. Meislin, M.D., Advisor
NYU School of Medicine Associate Professor of Orthopedic Surgery

Table of Contents

Table of Figures	5
Table of Tables	7
Authorship	8
Acknowledgements.....	9
Abstract.....	10
1. Introduction.....	11
2. Literature Review.....	13
2.1 Patellofemoral Joint Anatomy	13
2.1.1 Bones of the Knee	13
2.1.2 Musculature and Tendons	14
2.1.3 Cartilage and Bursae	15
2.2 Biomechanics.....	16
2.2.1 Patellar Biomechanical Function	16
2.2.2 Patellar Static Alignment	16
2.2.3 Patellar Dynamic Movement and Kinematics.....	18
2.2.4 Patellofemoral Joint Resultant Force	20
2.3 Disease States.....	21
2.3.1 Patellofemoral Arthritis.....	21
2.3.2 Chondromalacia	22
2.3.3 Quadriceps and Patellar Tendonitis	23
2.3.4 Malalignment	23
2.3.5 Lateral Compression Syndrome.....	24
2.3.6 Adolescent Hypermobility Patellofemoral Pain.....	24
2.4 Current Solutions and Limitations	25
2.4.1 Non-invasive	25
2.4.2 Semi-invasive.....	30
2.4.3 Surgical	30
2.4.4 Limitations of Current Solutions.....	31
2.5 Patents	31
2.5.1 Reaction Web Braces	31
2.5.2 Tendon Compression Strap.....	33
2.5.3 Air Brace	33
3. Project Strategy.....	35

3.1 Initial Client Statement	35
3.2 Technical Design Requirements	35
3.2.1 Design Objectives	35
3.2.2 Design Constraints	36
3.2.3 Design Operation and Components	37
3.3 Standard and Regulatory Design Requirements	37
3.4 Revised Client Statement	39
3.5 Management Approach	39
4. Design Process	41
4.1 Needs Analysis.....	41
4.2 Concept Maps	42
4.2.1 Initial Designs	42
4.2.2 Preliminary Design Analysis	45
4.2.3 Final Design Analysis	46
4.3 Design Calculations and Modeling	48
5. Design Verification	53
5.1 Methodology Summary	53
5.1.1 Skin Electromyography (EMG) Protocol.....	53
5.1.2 Nitrile Rubber Force Reduction – Force Plate Protocol	54
5.2 Summary of Data Collection and Analysis.....	54
5.2.1 Skin Electromyography Testing Results	54
5.2.2 Force Plate Testing Results.....	60
6. Final Design and Validation	63
6.1 Final Design Architecture	63
6.2 Design Validation	64
6.2.1 Skin Electromyography Validation.....	64
6.2.2 Force Plate Validation.....	65
6.2.3 Statistical Analysis.....	67
6.3 Impacts of Final Design	72
6.3.1 Economics.....	72
6.3.2 Environmental Impact.....	72
6.3.3 Societal Impact.....	73
6.3.4 Political Ramifications	73
6.3.5 Ethical Concerns	73
6.3.6 Health and Safety Issues	73

6.3.7 Manufacturability.....	74
6.3.8 Sustainability.....	74
7. Discussion.....	75
7.1. Project Limitations.....	75
7.1.1 Human Subject Limitations	75
7.1.2 Assumptions.....	75
8. Conclusion and Recommendations.....	76
8.1 Future Work.....	76
8.2 Conclusions.....	76
References.....	78
Appendices.....	83
Appendix A: Equations and Calculations	83
Appendix B: Skin Electromyography Protocol	85
Appendix C: Nitrile Rubber Force Reduction – Force Plate Protocol.....	86
Appendix D: Skin EMG Data	87
1. Rectus Femoris – Treadmill Testing (Average Maximum Peaks).....	87
2. Vastus Lateralis/Medialis – Treadmill Testing (Average Maximum Peaks).....	88
3. Rectus Femoris – Activity Testing (Average Maximum Peaks).....	89
4. Vastus Lateralis/Medialis – Activity Testing (Average Maximum Peaks).....	90

Table of Figures

Figure 1. Skeletal structures of the knee	14
Figure 2. Musculature of the quadriceps.....	15
Figure 3. Q-angle schematic	17
Figure 4. Patellar J-curve pattern of motion during knee flexion and extension.	19
Figure 5. PF joint forces, where F_p = patellar tendon force, F_q = quadriceps tendon force, R = PF joint resultant force	20
Figure 6. Stages of patellofemoral arthritis.....	22
Figure 7. Adjustable Patella Donut Brace.....	26
Figure 8. Tru-Pull Advanced System Brace	26
Figure 9. Reaction Web Knee Brace.....	27
Figure 10. Form Fit Knee Hinged Knee Brace	27
Figure 11. FX Patella Stabilizer Brace.....	28
Figure 12. Free Runner Knee Brace.....	28
Figure 13. Tendon Compression Strap	29
Figure 14. Web Framework Design, various views.....	32
Figure 15. Tendon Compression Strap	33
Figure 16. Adjustable Inflatable U-Shaped Air Cell Knee Brace	33
Figure 17. Front elevation view of the Orthopedic Brace with Inflatable Air Bag.....	34
Figure 18. Visual Analogue Scale (VAS) for evaluating pain levels.....	35
Figure 19. Gantt Chart for tracking project progress	40
Figure 20. Anti-Gravity Brace Design.....	43
Figure 21. Inflation Pocket Brace with Pullover Strap Design.....	44
Figure 22. Shock Absorbing Brace Design.....	45
Figure 23. Cuff component of brace prototype.....	47
Figure 24. Telescopic rod component of brace prototype.....	48
Figure 25. NBR component of brace prototype	48
Figure 26. Leg schematic without brace	48
Figure 27. Leg schematic with brace	48
Figure 28. Patellar forces without brace	49
Figure 29. Patellar forces with brace	49
Figure 30. Free body diagram without brace during knee flexion	49
Figure 31. Free body diagram with brace during knee flexion.....	50
Figure 32. Diagram showing the distance measurement	51
Figure 33. Example placement of electrodes on the rectus femoris (circled).....	53
Figure 34. Example placement of electrodes on the vastus medialis (circled in blue) and lateralis (circled in red).....	53
Figure 35. Example experimental setup for a treadmill run.....	54
Figure 36. Example raw dominant leg EMG signal data during running	55
Figure 37. Total average maximum peaks of rectus femoris (left) and vastus medialis/lateralis (right) EMG signals during running.	56
Figure 38. Example experimental setup for a squat.....	57
Figure 39. Example raw dominant leg EMG signal data during squats.....	58
Figure 40. A collection of graphs that show average maximum peak data during various activities.....	60
Figure 41. Vertical impact force values using a 5-lb weight versus time	61

Figure 42. Measured vertical impact force values (N) from NBR and no material test conditions using a 5-lb weight	61
Figure 43. Measured vertical impact force values (N) from NBR and no material test conditions using a 10-lb weight	62
Figure 44. Final design prototype	63

Table of Tables

Table 1. Classification of patellar tendonitis	23
Table 2. Pairwise Analysis Chart for ranking project objectives.....	41
Table 3. Pugh Analysis chart for final design selection.....	46
Table 4. Distance optimization data.....	52
Table 5. Average maximum peaks of EMG signals during running.....	56
Table 6. Average maximum peaks of EMG signal during squats.....	59
Table 7. Average maximum peaks of EMG signal during stairs	59
Table 8. Average maximum peaks of EMG signal during lunges	59
Table 9. Percent impact force reduced with increasing number of layers of NBR foam for the 5- and 10-lb weight tests	66
Table 10. Mean rectus femoris signal (Prototype Brace vs. No Brace).....	67
Table 11. Mean rectus femoris signal (Prototype Brace vs. Reaction Web Brace)	68
Table 12. Mean vastus medialis signal (Prototype Brace vs. No Brace)	69
Table 13. Mean vastus medialis signal (Prototype Brace vs. Reaction Web Brace)	69
Table 14. Mean vastus lateralis signal (Prototype Brace vs. No Brace)	70
Table 15. Mean vastus lateralis signal (Prototype Brace vs. Reaction Web Brace)	70
Table 16. Mean impact force, 5-lb Drop Test.....	71
Table 17. Mean impact force, 10-lb Drop Test.....	72

Authorship

All components of this Major Qualifying Project were equally contributed to by all members of the project team.

All chapters and sections of this report were equally contributed to and edited by all members of the project team.

Acknowledgements

This project was made possible with support from numerous individuals. We would sincerely like to thank them for their guidance, contribution, and dedication to our project.

We would like to thank our advisors, Professor Sakthikumar Ambady and Professor Ahmet Can Sabuncu, for their endless guidance and effort throughout the duration of this project. We thank both professors for the opportunity to allow us to develop as students, researchers, and designers. Additionally, we would like to thank Dr. Robert Meislin for enabling this project come to fruition, and for his knowledge, support, and time that he has dedicated to making this project a success.

We would also like to thank Thomas Partington, lab manager of the Goddard Hall Machine Shop, for his valued assistance in fabricating and manufacturing our device. Additionally, we would like to thank lab manager Lisa Wall for her reliability and accessibility during the project's production. Finally, we would like to express our gratitude to Professor Tiffany Butler, Professor Joseph Stabile, Professor Karen Troy, Professor Dirk Albrecht, and athletic trainer Shannah Dalton for their time in meeting with us to provide insight to our project's background.

Abstract

Patellofemoral (PF) pain syndrome (PFPS) is the most common form of knee pain in the United States. Studies have shown that PFPS accounts for 25-30% of knee injuries presented in sports medicine clinics. Additionally, 18 and 33% of knee injuries in male and female athletes, respectively, are attributed to PFPS. PFPS can be attributed to the PF joint compression force: the resultant patellar force exerted on the femoral trochlea. Current solutions to either treat or alleviate PF pain include arthroscopic surgery, kinesiology taping techniques, and patellar tracking braces. These modes of treatment are either costly or do not directly mitigate the PF joint compression force. Thus, the purpose of this project was to design a brace that reduces the patellar force on the trochlea during physical activity. Our preliminary results signify that our brace reduces this PF compression force during certain activities; however, additional testing is required to further validate this conclusion.

1. Introduction

Patellofemoral (PF) pain syndrome (PFPS) is an overarching term that describes anterior knee discomfort caused by insufficient and inflamed articular cartilage present between the posterior patella and femoral trochlea [1]. The degradation and inflammation of this articular cartilage results from the PF joint compression force: the resultant patellar force applied to the femoral trochlea. This resultant force is generated from the quadriceps (key muscles include the *vastus lateralis*, *vastus medialis*, and *rectus femoris*) tendon and patellar tendon forces. Jumping, running, sitting for extended periods of time, climbing stairs, and other activities can cause an excessive compressive force on the patellofemoral joint and contribute to the onset of PFPS. General musculoskeletal disorders affect an estimated 126.6 million Americans [2]. Many of these cases include patients in the elderly and inactive populations; however, a growing number of active children, adults, and elite athletes are developing PF pain as a result of prolonged, high-impact activity. Studies have found PFPS to account for 25-30% of knee injuries presented in sports medicine clinics [3] [4], as well as 18% and 33% of knee injuries in male and female athletes, respectively [5]. Although some athletes or younger individuals are willing to continue to engage in a high level of activity due to a high pain tolerance or eagerness to return to action [6], an estimated 74% of PFPS patients will limit or give up sports and other physical activity altogether [4]. While decreased activity and physical therapy can temporarily alleviate some of the pain, PFPS patients often experience some degree of discomfort for a long period afterwards. Recent studies have suggested that patellofemoral pain developed in a patient's younger years can also reduce their mobility and activity and lead to the onset of knee osteoarthritis and further complications, resulting in preventable, but increased, healthcare costs [7].

Presently, there is a lack of specialized, non-invasive, and cost-effective treatments for patellofemoral pain. Current patellar bracing and kinesiology taping solutions fail to reduce the compressive force on the patella, stabilize the joint, or properly ensure that muscles do not exhibit atrophy as a result of treatment. Due to the complex and largely interior characteristics of the patellofemoral joint, targeted, specialized solutions for PF pain, such as injections or surgery, are invasive. The invasive nature of these treatments can often be a source of hesitation for patients. Furthermore, surgery is often expensive and only a short-term solution. In 2015, it was estimated that more than \$27 billion in health care expenditures were attributed to knee-related pain [8].

Patients who opt for the surgical route pay thousands of dollars for an initial surgery and even more for subsequent revision surgeries. The absence of patellofemoral-specialized, non-invasive treatment, and growing cases of PFPS necessitates a targeted solution.

In hopes of providing a more specialized and cost-effective solution, the goal of this project was to design a shock absorbing brace that effectively targeted the patellofemoral joint and provided both pain relief and support to patients experiencing patellofemoral pain. The shock absorbing brace was designed to reduce the impact forces the patellofemoral joint is subjected to in an effort to reduce the compression force in that region. Since patellofemoral pain is prevalent in young and inexperienced athletes, it was important for the brace design to be versatile for a variety of activities and adjustable to fit to varying leg dimensions. Additionally, the brace needed to avoid causing skin injury and irritation and had to be wearable for longer periods of time. Once these design parameters were fulfilled, the goal was to fabricate a working prototype that would undergo testing to validate the effectiveness of the product.

The team designed a brace capable of alleviating patellofemoral pain caused by the friction between the patella and the femur. The device was adjustable to provide a customized fit for users of various sizes and was designed with a soft, yet durable material to prevent skin irritation while withstanding wear from physical activity. The knee brace also allowed for the patient to retain a large degree of normal range of motion. Furthermore, it enabled the muscles and bones to play a role in the movement of the knee joint so that patients did not weaken their muscles by completely relying on the brace. The prototyping of the brace was completed using SolidWorks, a computer aided design program, and manufactured using the facilities available at Worcester Polytechnic Institute.

Functional properties of the brace were tested through impact testing. The range of motion of an individual wearing the brace was also observed to ensure that the brace does not severely limit movement. Test subjects were also asked to wear the brace and rate its comfort, fit, and adjustability. The quantitative and qualitative data gathered were statistically analyzed using Excel and MATLAB to determine the brace's effectiveness. After this initial set of data was reviewed, improvements were made on the brace and the same tests were performed again to further validate the benefits of the brace and assess areas of future improvements.

Using the background knowledge collected, the team brainstormed several initial design prototypes. The needs and requirements for the brace were evaluated and a final design concept was chosen. A prototype of the design was fabricated and tested for validation. The results of the testing were discussed and recommendations for future work were made.

2. Literature Review

To enhance our understanding of the causes of patellofemoral pain and how a shock absorbing knee brace could alleviate it, the team conducted a literature review on knee anatomy and biomechanics, patellofemoral disease states, and the shortcomings of current treatments.

2.1 Patellofemoral Joint Anatomy

The knee is a highly complex mechanism that acts as a hinge, or lever-like joint that is responsible for most movement and stability of the leg. Situated between the distal thigh and proximal leg, the knee itself is made up of several bones, ligaments, tendons, muscles, and other structures. Accurate diagnoses and treatments of knee ailments necessitates a comprehensive understanding of its complex and intricate structures, which will be described in detail in subsequent sections.

2.1.1 Bones of the Knee

The femur is a long bone that makes up the thigh region. It is the largest and strongest bone in the body, and its asymmetrical structure allows it to withstand a great deal of stress, provide balance, and maintain a favorable center of gravity [9]. Proximally, the femoral head of the femur articulates with the pelvis, and the lateral greater trochanter and posteromedial lesser trochanter serve as sites of muscle attachment. At the distal end of the femur, the lateral and medial epicondyles serve as the site of attachment for the muscles and articulate with the tibia. The epicondyles are asymmetrical, allowing for proper extension and flexion of the knee [10].

Between the two epicondyles lies the femoral trochlea, where the femur articulates with the patella. The patella, shaped similarly to an upside-down triangle, is the largest sesamoid bone in the body; however, on average, it is only around 4 centimeters long, 5 centimeters wide, and 2 centimeters thick [11]. There is an incongruent fit of the patella in the patellofemoral joint, mainly due to the convex orientation of the patella's anterior-posterior and medial-lateral planes. The connection to the joint rests mostly on the articular cartilage on the patella's articulating surface, which can reach up to seven millimeters in thickness [11].

Like the femur, the tibia is also a long bone. As the second largest and strongest bone following the femur, the tibia distributes the weight from the upper body and the femur down towards the feet. It articulates distally with the talus bone of the foot [9], and articulates with the fibula on both ends; however, the fibula has little involvement in the movement of the knee.

Ligaments are bundles of fibrous connective tissue that connect bone to bone. The knee has four main ligaments (shown in Figure 1) that weave through spaces in the joint to connect the femur to the tibia: the anterior cruciate ligament (ACL), posterior cruciate ligament (PCL), medial collateral ligament (MCL), and the lateral collateral ligament (LCL). The ACL and PCL cross each other to form an “X”, controlling translation and rotation of the tibia. The MCL and LCL provide stability to the medial and lateral sides of the knee, respectively [12].

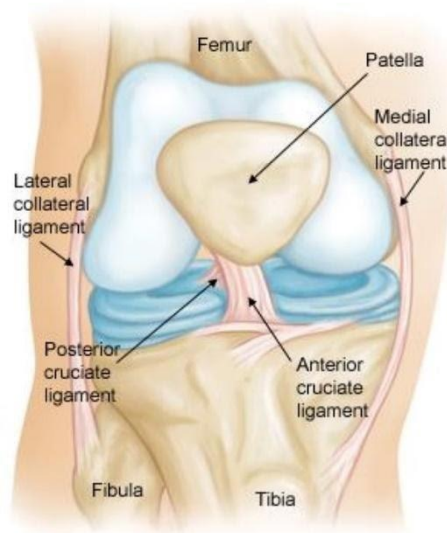


Figure 1. Skeletal structures of the knee

(Source: <https://orthoinfo.aaos.org/en/diseases--conditions/collateral-ligament-injuries/>)

The bony structures of the knee make up two main joints, the femorotibial and patellofemoral joints. Working in conjunction, these components allow the leg to have six degrees of motion in three different planes [13].

2.1.2 Musculature and Tendons

There are two main groups of muscles involved in knee movement: the hamstring group and the quadriceps femoris [9]. The hamstrings are located on the posterior thigh and consist of a group of three muscles: *biceps femoris*, *semitendinosus*, and *semimembranosus*. The quadriceps femoris is located on the anterior thigh and consist of a group of four muscles, shown in Figure 2: *rectus femoris*, *vastus lateralis*, *vastus medialis*, and *vastus intermedius*.

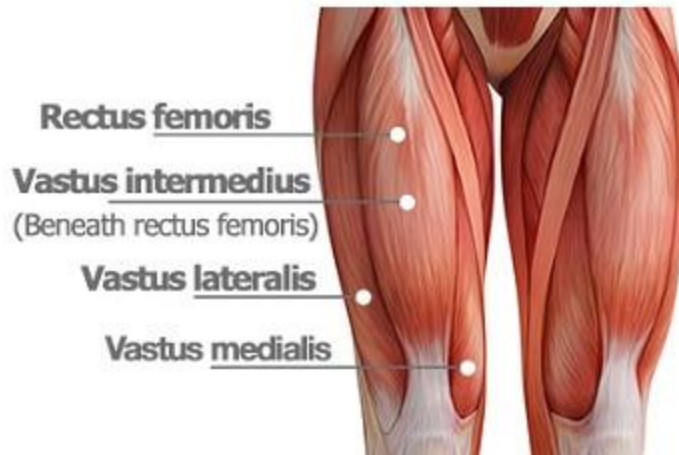


Figure 2. Musculature of the quadriceps

(Source: <https://www.knee-pain-explained.com/kneemuscles.html>)

Knee extension and knee strength are largely attributed to the *quadriceps femoris*, and thigh extension and knee flexion is largely attributed to the hamstring muscles [9]. The medial musculature of the knee, composed of the sartorius and gracilis muscles, and the lateral musculature, composed of the iliotibial band and the popliteus, also aid in knee flexion to a small degree. Several muscles, such as the biceps femoris and popliteus, are involved in the lateral and medial rotation of the knee [13].

These muscles are connected to the bones of the knee via tendons. Tendons, like ligaments, are bundles of fibrous connective tissue. The main tendon of the knee is a continuous structure consisting of two regions: the quadriceps and patellar tendons [14]. Connecting the quadriceps muscles to the patella, the quadriceps tendon helps extend the leg at the knee, and the patellar tendon, also called the patellar ligament due to its connections from the patella to the tibia, primarily functions to prevent unwanted movement and tracking of the knee [14].

2.1.3 Cartilage and Bursae

The femoral and tibial condyles are covered with articular cartilage, a highly specialized type of connective tissue that allows for smooth movement between bone surfaces and serve as shock absorbers during movement [13]. Articular cartilage lacks nerves and is nonvascularized, therefore having little to no natural healing or repairing capabilities [15]. With time and use, articular cartilage inherently wears down, leading to bone-on-bone rubbing that can cause pain.

Between the medial and lateral femoral condyles and the proximal tibia, the white, fibrocartilaginous meniscus is made up of medial and lateral components that allow the tibial condyles to “sit” on the corresponding femoral condyles [13]. Menisci are critical to a healthy knee joint and aids in joint lubrication, shock absorption, and load transmission.

The knee contains several bursae, which are sacs filled with synovial fluid. This fluid reduces friction between articular surfaces in the body, such as bone and muscle, and skin and muscle. There are four located on the frontal and medial faces of the knee and four on the lateral side of the knee, generally in locations of high friction and high motion [13]. Inflammation of these fluid sacs, referred to as bursitis, is often caused by blunt trauma, infection, or overuse. Around the patella lie the prepatellar bursa, superficial and deep infrapatellar bursae, and the suprapatellar bursa [16].

2.2 Biomechanics

One of the leading factors that causes patellofemoral joint pain is biomechanical dysfunction. The articulation of the patella and femoral trochlea is anatomically specific to each individual, and for some, the patella may improperly align or track within this joint. Additionally, the biomechanical function of the patellofemoral joint is dependent upon a balance of forces generated from the surrounding soft tissue structures. Unbalanced forces from these structures can result in an augmented force distribution between the posterior patella and femoral trochlea, known as the patellar compression force. This causes persistent pain in this anatomical region [11].

2.2.1 Patellar Biomechanical Function

The principal biomechanical function of the patella is to act as a mechanical pulley for the quadriceps as it changes the direction of the extension force throughout the range of motion of the knee. Furthermore, the patella displaces the patellar tendon away from the femorotibial contact point throughout the knee range of motion, thus increasing the patellar tendon moment arm. In addition to acting as a mechanical pulley, another key biomechanical function of the patella is to concentrate the divergent forces originating from the four heads of the quadriceps during flexion and transmit these tensile forces in a frictionless manner around the femur to the patellar tendon and tibial tuberosity [11].

2.2.2 Patellar Static Alignment

The static alignment of the patella is dependent on the depth of the femoral sulcus, the height of the lateral femoral condyle, and the specific geometric orientation of the patella. In full extension, the patella possesses a slight lateral deviation anterior to the lateral femoral condyle, when observed in the frontal plane. The patella is most mobile when the knee is in full extension. When the knee is fully extended, the patella is positioned superior with respect to the trochlea and makes minimal contact with the articular surface of the trochlea.

The Q-angle is clinically used to assess the overall lateral direction and magnitude of the line of pull (originating from the anterior superior iliac spine to the mid-patella) of the quadriceps relative to the

patella. It is measured by the angle between the line of pull of the quadriceps and a line connecting the center of the patella with the tibial tuberosity, shown in Figure 3.

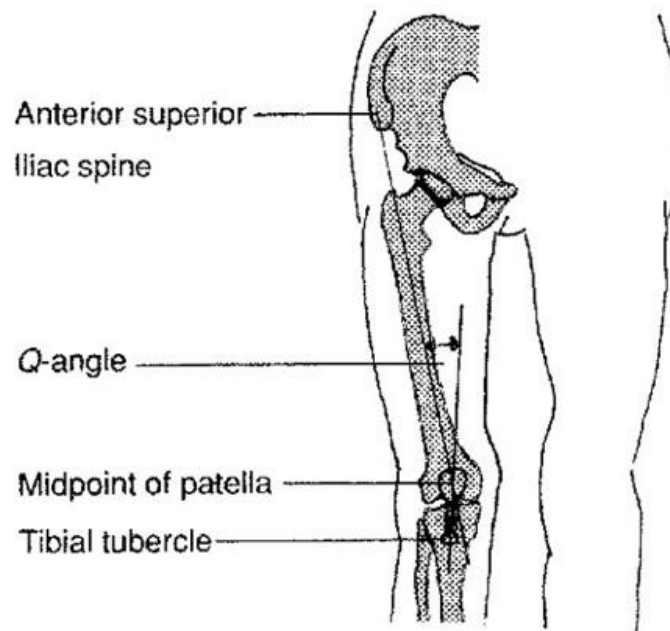


Figure 3. Q-angle schematic

(Source: <http://www.yourskicoach.com/glossary/SkiGlossary/Edging.html>)

A normal Q-angle ranges from 10-13 degrees for males and 15-17 degrees for females. It is believed that an increased Q-angle will produce disproportionate lateral forces on the patella, causing it to be pulled to the lateral side of the trochlea, a phenomenon known as the bowstring effect [11].

In the sagittal plane, the apex of the patella is situated at, or slightly proximal, to the joint line when the knee is in slight flexion. A more advanced procedure to measure the sagittal plane position of the patella is to utilize the Insall-Salvati ratio. This value quantitatively represents the ratio of the length of the patellar tendon compared with the height of the patella at 30 degrees of flexion. An Insall-Salvati ratio around 1.0 is considered normal. A ratio less than 0.80 indicates that the patient likely has an inferior patella, known as patella baja. A ratio greater than 1.20 indicates that the patient likely has a superior patella, known as patella alta. For patients with patella alta, it requires more time for the patella to reach the bony constraint of the trochlea, resulting in a higher probability of subluxation [11].

Furthermore, in static alignment, the patella should be vertically positioned so that the inferior and superior borders are equidistant from the trochlea. The patella exhibits tilt if it deviates anteriorly or posteriorly within the joint. In the sagittal plane, these deviations are characterized by the location of the inferior border of the patella in either an elevated (superior tilt) or depressed (inferior tilt) position. An

inferior tilt can be troublesome for the patient as it may cause pinching or irritation of the patellar fat pad located posterior to the patellar tendon. In the transverse plane, the patella should be horizontally positioned so that the medial and lateral borders are equidistant from the trochlea. A medial tilt occurs when the lateral border is superior to the medial border. On the other hand, a lateral tilt occurs when the medial border is superior to the lateral border, resulting in lateral patellofemoral compression syndrome [11].

The rotation of the patella occurs around the anterior-posterior axis and is characterized by the rotational direction of the inferior border of the patella. A medial patellar rotation occurs when the inferior border of the patella is directed medially, whereas, a lateral patellar rotation occurs when the inferior border of the patella is directed laterally [11].

2.2.3 Patellar Dynamic Movement and Kinematics

Since patellofemoral pain is predominant while the patella is in motion, it is crucial to understand the dynamic and kinematic principles involved in the process of patellar tracking. Patellar tracking during tibiofemoral motion is contingent on the geometries of the patella and trochlea, the magnitude of the active contractile forces from the quadriceps, and the extensibility of the articular connective tissue surrounding the patella within the patellofemoral joint. Within this gliding joint, the patella demonstrates motion in multiple planes. These motions include a medial or lateral glide, medial or lateral tilt, medial or lateral rotation, and a superior or inferior glide. A superior glide, known as patellar extension, occurs during tibiofemoral extension when the quadriceps contract causing a superior pull on the patella. An inferior glide, known as patellar flexion, occurs simultaneously with tibiofemoral flexion. Lateral and medial glides occur as translations in the frontal plane that coincide with tibiofemoral pain. During a medial glide, the medial patella moves towards the medial side of the knee, whereas in a lateral glide, the lateral patella moves closer to the lateral side of the knee. A patellar tilt occurs about the longitudinal axis. More specifically, patellar tilts are described by which direction the reference facet is moving towards. For example, in a medial tilt, the medial posterior facet migrates toward the medial femoral condyle. Similarly, in a lateral tilt, the lateral posterior facet migrates toward the lateral femoral condyle [11].

During open chain motion of the knee, the patella follows the path of the tibia because of the distal insertion of the patellar tendon to the tibial tubercle. The patella glides superiorly during knee extension and inferiorly during knee flexion. As the knee experiences flexion, the articulating surface of the patella varies throughout the range of motion. The contact point moves proximally along the patella and inferiorly-posteriorly along the medial and lateral femoral condyles. Patellar contact area increases as the degree of knee flexion increases, which helps distribute the joint forces over a greater surface area, resulting in a reduced normal stress on the patella. In patients with proper patellofemoral joint alignment,

this force distribution allows the knee to withstand the damaging effects that could occur from constant exposure to high joint compression forces [11].

As the knee undergoes flexion, the inferior portion of the patella makes contact with the superior portions of the femoral condyles. This contact is initiated between the lateral facet of the patella and the lateral femoral condyle. By 30 degrees of flexion, the contact is evenly distributed on both sides of the femoral condyles with a total contact area of approximately 2.0 cm². The contact area is initially small and progressively increases as the joint becomes more congruent. At 60 degrees of flexion, the superior patella makes contact with the trochlea slightly inferior to the area of contact at 30 degrees of flexion. The contact area between the posterior patella and trochlea continues to increase as the knee flexes to 90 degrees and is approximately equal to 6.0 cm². At 90 degrees of flexion, the superior patella makes contact with the area of the trochlea just above the femoral notch. Between 90 and 120 degrees of flexion, the superior patella makes contact with the area of the trochlea surrounding the intercondylar notch. In deep knee flexion, the patella links the span of the intercondylar notch and there is contact only on the extreme medial and lateral sides of the patella. At full flexion, the only articulating contact occurs between the odd facet of the patella and the lateral surface of the medial femoral condyle [11].

In addition to exhibiting superior and inferior motions during knee range of motion, the patella tracks lateral-medial-lateral during tibiofemoral extension and flexion. In a normal knee, there is slight excessive medial or lateral motion that occurs during flexion since the patella is relatively centered on the trochlea. It is also important to note that when the knee is in full extension, the patella is positioned slightly lateral because of the tibia's external rotation. The approximate amount of medial and lateral displacement is equivalent to 3 mm in each direction. As the knee undergoes flexion, the patella glides medially and centers itself within the trochlear groove following a J-curve motion pattern, evident in Figure 4.



Figure 4. Patellar J-curve pattern of motion during knee flexion and extension.

(Source: <https://pubmed.ncbi.nlm.nih.gov/17263214/>)

When the knee extends from 45 to 0 degrees, the patella tilts medially about 5 to 7 degrees from a laterally tilted position related to the geometric orientation of the trochlea. At 30 degrees of flexion, the patella glides back to the lateral side where it maintains this lateralization for the rest of the knee flexion [11].

In closed kinetic chain movements, the patella is tethered within the quadriceps tendon. As the femur rotates in the transverse plane, the surface of the femur glides behind the patella. When there is excessive femoral internal rotation, the lateral facet of the patella migrates towards the lateral anterior femoral condyle. An increase in the hip internal rotation, also known as hip adduction, has been proposed as a potential risk factor for patellofemoral pain.

2.2.4 Patellofemoral Joint Resultant Force

The patellofemoral joint resultant force (R), evident in Figure 5, is the resultant compression force acting on the joint and is responsible for causing patellofemoral pain syndrome in patients. Biomechanically, this is the resultant force of the quadriceps tendon (F_Q) and patellar tendon (F_P) and thus is directly dependent upon the magnitude of these tendons' forces within the patellofemoral joint.

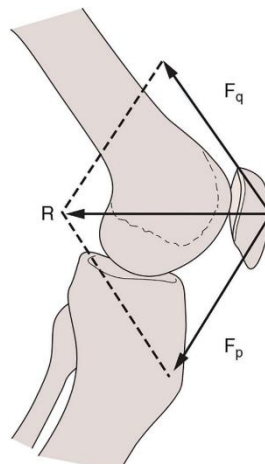


Figure 5. PF joint forces, where F_p = patellar tendon force, F_q = quadriceps tendon force, R = PF joint resultant force

(Source: <https://www.ncbi.nlm.nih.gov/pmc/articles/PMC5095937/>)

The normal stress placed on the patellofemoral joint is calculated by dividing the patellofemoral joint reaction force by the patellofemoral joint contact area. This stress value represents the joint stress measured as a force per unit area. As the contact area between the posterior patella and trochlea increases, the normal stress exerted on the patellofemoral joint decreases. Conversely, a high patellofemoral joint reaction force linked with a small contact area between the posterior patella and trochlea will result in a high patellofemoral joint stress that may be detrimental to the surrounding joint cartilage. Furthermore,

this patellofemoral joint stress can be exacerbated with poor patellar positioning within the trochlea. Since the point of contact between the posterior patella and trochlea varies throughout the knee range of motion, the patellofemoral joint reaction force changes because of changes in the lever system of the knee. In non-weight bearing situations, the contact area between the posterior patella and trochlea increases as the knee undergoes flexion from 0 to 90 degrees. Therefore, the patellofemoral joint stress decreases as the degree of knee flexion increases [11].

When the foot is placed in a fixed position, the patellofemoral joint reaction force increases as knee flexion decreases from 90 to 45 degrees, then decreases as the knee reaches full extension. The patellofemoral joint reaction force and joint stress can induce pain even in the most basic activities of daily life, not to mention in sports and recreational activities. To put patellofemoral joint forces into perspective, studies have measured joint forces 1.3 times the body weight during level ambulation, 3.3 times the body weight during stair ambulation, 5.6 times the body weight during running, and up to 7.8 times the body weight while squatting or deep knee bending [11].

2.3 Disease States

There are a number of disease states and conditions that can cause patellofemoral pain and discomfort. These can affect the articular cartilage protecting the femur and patella, the tendons surrounding the patella, the location of the patella, or even the patellofemoral joint itself. Athletes are particularly at risk for these types of diseases or conditions, as certain movements or overuse can cause further aggravation.

2.3.1 Patellofemoral Arthritis

Patellofemoral arthritis specifically affects the patellofemoral joint and is caused by the osteochondral degeneration of the joint. This means that there is damage to the articular cartilage that covers the bone, as well as damage to the bone itself. In healthy knees, the articular cartilage has an average thickness of 7-8 millimeters [17]; however, with patellofemoral arthritis, the articular cartilage is significantly diminished. Since the articular cartilage acts as a shock absorber between the patella and the femur, this lack of protection can lead to unintended contact between the patella and femur. In addition to inflammation and degeneration to the articular cartilage, abnormal tracking of the patella in the trochlear groove is also often associated with patellofemoral arthritis.

This combination of patellar maltracking and degeneration of cartilage can lead to a great deal of pain. Patellofemoral arthritis is often characterized by anterior knee pain that is further aggravated by activities that increase flexion in the knees. This increased flexion leads to a larger force load on the patellofemoral joint and causes more pain. Some of these activities include standing up, sitting down,

walking uphill, stairs, and kneeling. Patellofemoral arthritis can also cause popping, cracking and grinding sounds in the knee.

Patellofemoral arthritis is a common condition within the United States. About 14 million people suffer from some form of osteoarthritis in their knees, and half of this population reports pain in the patellofemoral area [17]. Increased risk for patellofemoral arthritis includes age, obesity, previous patellar fracture, prior dislocation or subluxation, history of arthritis in other joints, and overuse during high impact sports.

Computed tomography (CT) scans can be used to better assess the patellofemoral joint. However, this is often seen as unnecessary if arthritis is suspected. More commonly, it is used to identify lateral patellar subluxation or femoral trochlear dysplasia as opposed to checking for patellofemoral arthritis. In the event that a CT scan is taken, the arthritis can be classified into three basic stages: mild, moderate, and severe, shown by Figure 6. It is classified as mild if there is more than 3 mm of joint space, moderate if there is less than 3 mm of joint space but no bony contact, severe if the bony surfaces are in contact over less than one-quarter of the joint surface, and is considered very severe when the bony contact is over the whole joint surface [17].



Figure 6. Stages of patellofemoral arthritis

(Source: <https://orthoinfo.aaos.org/en/diseases--conditions/patellofemoral-arthritis/>)

2.3.2 Chondromalacia

Chondromalacia (also known as sick cartilage) is a condition that affects cartilage at the articular surface of bone and often results in tears, fissures and erosions of the cartilage. This can occur in any joint, but joints that have had trauma or defects are more prone to the development of chondromalacia [18]. The patellofemoral joint is the most common joint that is affected by chondromalacia, and in this location, the condition is known as chondromalacia patella, patellofemoral syndrome or runner's knee. In this case, the cartilage that cushions the patella against the trochlear groove becomes damaged.

Chondromalacia and patellofemoral arthritis are very similar, as they both cause anterior knee pain and are worsened by similar types of activities, such as stair climbing, running, and hiking. Chondromalacia is usually classified using the Outerbridge Classification to identify the severity of cartilage damage. Level

1 indicates the softening of the cartilage, Level 2 indicates more advanced degradation, Level 3 indicates fissuring of the cartilage down to the subchondral bone and Level 4 indicates the most severe and refers to a completely exposed bone. An arthroscopy of the knee is usually done to identify the level of chondromalacia.

2.3.3 Quadriceps and Patellar Tendonitis

Tendonitis occurs when a tendon becomes inflamed due to microscopic tears. These microscopic tears are often a result of a sudden or heavy tensile load on the affected tendon, as well as overuse of the tendon [19]. The quadriceps and patellar tendons are commonly affected by tendonitis, and the condition is often referred to as “jumper’s knee”. This condition is very frequent among athletes, more specifically those who play basketball and volleyball along with those who participate in long or high jump events [20]. The percentage of volleyball players affected by jumper’s knee ranges from 30 to 51% while that of basketball players ranges from 25 to 32% [21].

In patellar tendonitis, the proximal attachment of the patellar ligament is affected, resulting in pain, swelling or localized tenderness below the knee [20]. The pain must first be differentiated from similar disorders, like chondromalacia, and then can be classified into four stages. According to Table 1 [22], the four stages range from intermittent pain after sports in Stage 1, to a complete rupture of the patellar tendon in Stage 4 [20].

Table 1. Classification of patellar tendonitis

Stage	1	Pain only after sports
	2	Pain at the beginning of sports disappearing after a warm-up but reappearing with fatigue
	3	Constant pain at rest and with activity
	4	Complete rupture of the patellar tendon

2.3.4 Malalignment

Patellofemoral pain is influenced by malalignment of the patella relative to the patellofemoral joint. This pain is triggered by a joint reaction force being dispersed to the patellofemoral joint, and this irregular force subsequently causes pain in the compartment. Malalignment of the patella can take the form of maltracking, subluxation or dislocation. The dominant motion that the knee performs is active flexion and extension, and due to the anatomy of the knee, the center of rotation is proximal to the joint [23]. When the patella is misaligned, it is misaligned in a translational or rotational manner that leads to

forces being propagated over the patellofemoral joint and causing pain. Though medial subluxation is also largely associated with malalignment issues, lateral misalignment of the patella is the main cause of concern for PF pain due to the knee's proximal musculature.

Patellar tracking refers to the alignment of the patella in relation to the trochlear groove and during motion. Correct tracking of the patella is determined by the patella's position in the patellofemoral joint, and how the patella and trochlear groove's shapes align with one another [24]. Additionally, tracking is determined by the direction and magnitude of the forces from the quadriceps while the body is in motion [24]. When these factors are disrupted, maltracking of the patella in the trochlear groove can be observed and pain will subsequently occur.

2.3.5 Lateral Compression Syndrome

Pain in the knee can be caused by specific directional forces in the knee. When "lateral pressure in flexion" (LPIF) is present, chronic knee pain develops anteriorly due to the overloading of the lateral tissue. LPIF is localized on the lateral patellar facet when the knee is in flexion and pain results from the patella compressing the lateral side of the trochlear groove [25]. LPIF can be diagnosed by physicians, and is confirmed with a variety of symptoms, such as feelings of tenderness at the medial joint line of the patella accompanied by patella stability when the knee is in flexion and extension.

There are a few contributing factors to the pain that occurs in patients with lateral compression syndrome. A common factor may be prolonged knee flexion during everyday activity. Pain can also be prevalent during knee extension or can cause the knee to not reach full extension. Many patients will experience pain when sitting and at rest, as this position naturally bends the knee at 90 degrees of flexion. Most patients have a limited extension with LPIF along with chronic pain. This pain usually does not subside with medication, physical therapy, or bracing. Some means of pain relief can be achieved through clinical manipulation of the patella. Physicians can push the patella medially to be centered in the trochlea, which can provide instant relief for patients. With this manipulation, the tension in the surrounding ligaments is eased, and full extension can usually occur.

2.3.6 Adolescent Hypermobility Patellofemoral Pain

Generalized joint hypermobility is the ability of joints to move beyond the normal range of movement, both passively or actively [26]. It is hypothesized that this excess range of motion could be due to repetitive soft tissue microtrauma; however, this theory has not been proven, and in most individuals, the hypermobility of joints exists in isolation with no other issues [27]. Children and adolescents tend to have a greater range of motion in their joints when compared to adults, as range of

motion seems to diminish with age. As a result, hypermobility is a more common problem in children and adolescents, rather than adults [28].

Patellofemoral knee pain is the most common musculoskeletal pain in adolescents with hypermobile joints [29]. These individuals feel pain after physical activities such as standing, sitting, bicycle riding, or stair climbing. This pain can be caused by hypermobile patella, weak quadriceps muscles, malalignment of the patella, chondromalacia, subluxation, or even recurrent sprains in combination with joint hypermobility [28].

According to the Beighton Scale, a scale used to score generalized joint hypermobility, knees joints are considered hypermobile when there is a hyperextension greater than 10 degrees [27]. Generalized joint hypermobility may also present other symptoms such as easy bruising, atrophy scar formation, mild skeletal deformities and early onset osteoarthritis.

2.4 Current Solutions and Limitations

Since patellofemoral pain can be caused by medical conditions or simply be a result of an individual's knee joint structure, various methods are available on the market that can help alleviate the pain.

2.4.1 Non-invasive

Various knee braces available on the market provide patellofemoral support, whether that is through patella realignment or load dispersal through the joint. Three well-known brace companies, DonJoy, Ossur, and Breg, provide different-styled braces that help alleviate patellofemoral pain, which will be discussed further. Other non-invasive methods of decreasing patellofemoral pain include muscle taping, which can be self-taught and can provide an individualized solution for each patient. Lastly, some patients' pain and comfort can be relieved through simple remedies, such as a specific physical therapy routine or rest.

Knee braces are most commonly used to treat PF pain because they can be easily purchased and are available in multiple designs that can provide support for varying conditions. DonJoy's neoprene sleeve Adjustable Patella Donut Brace, shown in Figure 7, provides full-circumference support for patellar chondromalacia, patella tracking and patellar tendonitis. An adjustable buttress composed of rubber offers proximal, distal, medial, and lateral stability to the knee cap. The neoprene material provides compression and warmth, while the Drytex fabric makes the brace breathable to ensure comfort.



Figure 7. Adjustable Patella Donut Brace

(Source: <https://www.djoglobal.com/products/DonJoy/adjustable-patella-donut>)

The Tru-Pull Advanced System Brace relieves pain caused by patellofemoral dysfunction, lateral malalignment, and patellar tendonitis. This brace, shown in Figure 8, has an elastic strap that actively pulls the patella when the knee extends, and its independent anchors prevent it from rotating. It is also fabricated using a breathable material, making the brace light and comfortable [30].



Figure 8. Tru-Pull Advanced System Brace

(Source) <https://www.djoglobal.com/products/DonJoy/tru-pull-advanced-system>)

The Reaction Web Knee Brace, shown in Figure 9, incorporates an elastomeric web design that distributes energy across the knee, thereby reducing pain. The web mechanism is said to absorb shock and transfer high loads away from the area of the knee that is experiencing pain. This structure also stabilizes the patella and relieves pain due to patellofemoral instabilities. The open web network and the adjustable

straps above and below the knee offer a flexible and adjustable fit. The padded backing of the knee brace, which is made with a breathable lightweight material provides the necessary comfort for the wearer [31].



Figure 9. Reaction Web Knee Brace

(Source: <https://www.djoglobal.com/products/DonJoy/reaction-web-knee-brace>)

The Form Fit Knee Hinged Lateral J Brace from Ossur realigns and stabilizes the patella and provides lateral support if needed. The brace, shown in Figure 10, is intended for individuals suffering from lateral patellar subluxation and dislocations, lateral patellofemoral malalignment, patellofemoral maltracking and pain, and chondromalacia due to lateral maltracking [32].



Figure 10. Form Fit Knee Hinged Knee Brace

(Source: <https://www.ossur.com/en-us/bracing-and-supports/knee/formfit-hinged-knees>)

The FX Patella Stabilizer Brace is ideal for conditions such as patellofemoral pain syndrome, patellofemoral stress syndrome, patellar subluxation or dislocation, chondromalacia, and patellar

tendonitis. The brace helps control the frontal plane of the knee while allowing for extension and flexion. It comes with an adjustable thigh and frontal strap to allow for a customizable fit, as shown in Figure 11. Additionally, the brace is made of Coolflex, which is a breathable fabric that reduces perspiration while the brace is kept tightly around the leg [33].



Figure 11. FX Patella Stabilizer Brace

(Source: <https://www.ossur.com/en-us/bracing-and-supports/knee/fx-patella-stabilizer>)

Breg's Free Runner Knee Brace is intended for individuals who suffer from patellofemoral pain due to maltracking, subluxation, or knee injuries. Its design includes a patent-pending CAM hinge that provides dynamic support and is made with a Smart-Zone compression fabric that is lightweight and discrete. The Free Runner Knee Brace, shown in Figure 12, provides compression when the knee is fully extended and relaxes during flexion to allow full range of motion. The inside of the brace contains a lateral buttress that stabilizes and centers the patella [34].



Figure 12. Free Runner Knee Brace

(Source: <https://www.breg.com/products/knee-bracing/patellofemoral/freerunner-knee-brace/>)

The Tendon Compression Strap, shown in Figure 13, is intended to help reduce inflammation of the patellar tendon. The low-profile, neoprene strap is commonly used for patellar tendonitis and chondromalacia. It includes a padded buttress for compression and has padding under the buckle for support [35].



Figure 13. Tendon Compression Strap

(Source: <https://www.breg.com/products/knee-bracing/patellofemoral/tendon-compression-strap/>)

Similar to knee braces, patellofemoral taping helps decrease pain and enables muscle-strengthening exercises to be performed correctly. Taping allows the individual to position the patella accordingly so when the knee bends, it does not cause pain as it glides against the femur. Initially, a piece of Hyperfix tape is placed directly over the kneecap to act as an anchor point for additional strips. Depending on how the patella needs to be supported, the kneecap can be tilted superiorly, anteriorly, laterally or proximally [36]. Taping can be done by a psychotherapist or can be self-taught. The type of sports tape used can be purchased over-the-counter from local pharmacies, and depending on the frequency of use, one package can last between 40 and 60 days. Hypoallergenic underlay tapes are often used when taping to prevent skin irritation [37]. Taping generally inhibits the knee's full range of motion, as excessive movement can cause the tape to detach. Additionally, the tape will need to be reapplied over time since its effectiveness will decrease with increased stretching [36]. One study showed that individuals with patellofemoral joint osteoarthritis who wore the tape experienced less immediate pain and the malalignment of their patella was reduced. Further research needs to be completed to determine the long-term effects of patella taping [38].

Conservative treatment is another beneficial treatment method for individuals suffering from patellofemoral pain. Rest, changes in physical activity, and cold compresses are important components of

the initial treatment. Anti-inflammatory medicine and orthotics that can also be purchased directly by the patient without a prescription can alleviate pain. Physical therapy can also remediate some of the pain. Strengthening the quadriceps and increasing quadricep and hamstring flexibility can help reduce some of the patella pain. Hip stability and strengthening are also crucial; hip extensors can absorb 25% of the energy released during step-off landing. If the hip muscles are not strong enough, this energy will be absorbed by the lower extremities, mainly the knee joint [39].

2.4.2 Semi-invasive

Patients whose pain is not alleviated with the aid of braces, taping, physical therapy regimens, or oral medication may receive corticosteroid or hyaluronic acid injections to relieve patellofemoral pain [39]. Corticosteroids, usually known as glucocorticoids, are a type of steroid hormones that are released by the adrenal cortex. They regulate cellular functions such as development, homeostasis, metabolism, cognition, and inflammation. They are a common treatment for inflammatory diseases [40]. Hyaluronic acid is found in the knee joint and enables synovial fluid to maintain its viscoelastic properties. When the concentration of hyaluronic acid decreases due to joint complications, the knee starts to lose its mechanical properties. Through hyaluronic injections, the synovial fluid regains its viscoelasticity, is able to aid in shock absorption, and can protect and lubricate the knee joint again [41].

2.4.3 Surgical

Operative procedures are generally used as a last resort in patients with patellofemoral pain. Generally, older individuals who experience severe pain or whose articular cartilage has been almost entirely worn out resort to this treatment option. There are two common procedures that can be performed: a patellofemoral joint replacement or a distal realignment or unloading procedure. Patellofemoral joint replacement, also known as partial knee replacement, is an operative procedure for individuals who suffer from patellofemoral arthritis. During the surgery, the damaged cartilage and a small amount of bone is removed from the patella and the groove on the femur. The removed region from the patella is replaced with a high-density plastic patella, and a metal laminate is placed in the groove of the femur, reducing the friction between the patella and the femur.

Distal realignment or unloading procedures, which are the most popular surgical procedures, move the tibial tubercle to offload the patellofemoral articulation. The first operation, known as the Elmslie-Trilliant procedure, is ideal for patients who suffer from lateral patellar subluxation or dislocation but who do not have patellofemoral articular damage. This operation aims to move the tibial tubercle medially without offloading the articular surface. Studies completed on the success of this procedure conclude that it reduces concurrent instability and improves knee function. The unloading procedure is a

modification of the previously mentioned operation; it includes anteriorization of the tubercle up to 15 mm, which reduces the lateral facet contact pressure. This procedure is recommended for patients who experience patellofemoral pain as a result of chondromalacia patella. Articular abnormalities are generally found on the distal medial or central lateral patellar facets. The procedure's goal is to reduce lateral facet contact pressure. If the patient has a lateral patellar tilt, a lateral release can be performed too, which can offload forces from the distal and lateral facets and transfer them to the proximal medial facet [39].

2.4.4 Limitations of Current Solutions

Knee braces help compress the patella to prevent maltracking and malalignment. They can also provide lateral support that prevents the patella from shifting during exercise. Unloader knee braces claim to have the ability to distribute loads across the knee joint to reduce high loads from being placed on one specific area; however, these braces share many similarities with compression braces, which solely focus on correcting knee alignment. Muscle taping can provide a more customizable solution than a standard knee brace, but this solution is temporary and necessitates replacement as the tape's strength decreases with use.

Injections are a semi-invasive treatment option that may not be as beneficial as they may seem and can cause further health complications. Clinical trials, reviews and meta-analyses do not provide clear conclusions on the effectiveness of hyaluronic injections when compared to a placebo, indicating that further research must be conducted [41]. Additionally, there are adverse effects to taking corticosteroids injections; extremely high doses can cause osteoporosis, skin atrophy, or diabetes, among other medical complications. Likewise, patients who have taken corticosteroid injections for prolonged periods of time can develop a resistance to it, which would decrease the drug's effectiveness [40]. Similarly, operative solutions are invasive, require additional time for recovery and can be costly if not covered by medical insurance. Partial joint replacement is an invasive procedure and patients will generally need 6-12 months to achieve a full recovery which is dependent on the restoration of the muscle strength.

2.5 Patents

To better develop a novel final design, researching current braces that help alleviate patellofemoral pain was necessary. Having a better understanding of existing designs and patents also ensures more familiarity with the patent process, which is another step in the scope of this project.

2.5.1 Reaction Web Braces

Several designs similar to the Reaction Web Knee Brace have been patented. These braces, illustrated below in Figure 14, are composed of a lateral upright and two semi-rigid structures that support the knee and are connected by a hinge. These also have a cuff that goes around the patient's thigh and calf

that is constructed out of a moldable material that can be changed according to the individual's leg dimensions. The brace also has the elastomeric web-like structure that is adjustable through a tension mechanism [42].

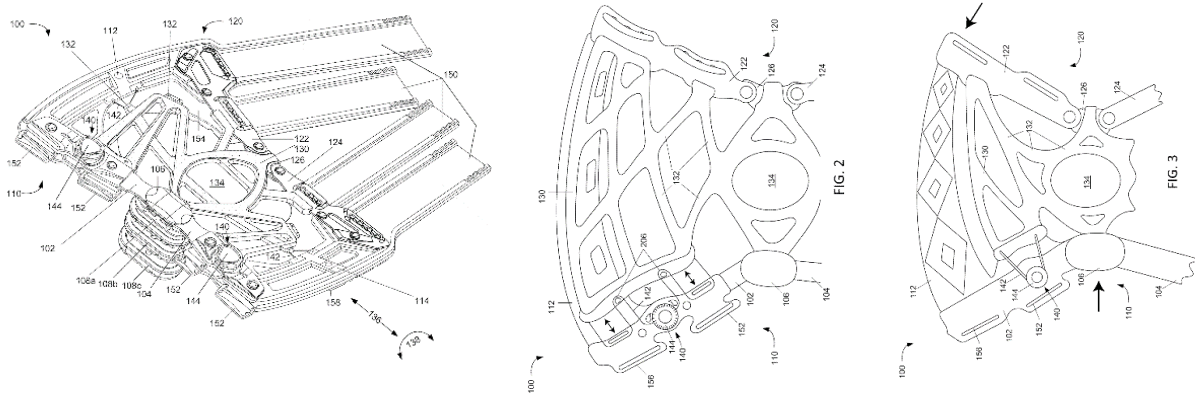


Figure 14. Web Framework Design, various views

(Source: <https://patents.google.com/patent/US20170105865>)

The brace claims to be used in the treatment of osteoarthritis. A condyle pad is attached to the hinge so it prevents it from contacting the patient's skin. A strap along the posterior of the knee secures the brace to the patient's leg. One adjusting element is incorporated into the tension mechanism. This element can be one of the following tension mechanisms: a reel-and-lace, a lever, a screw, a lace-and-cleat, buckles, a post-and-strap, a hook-and-loop, and a notched band-and-pawl [42]. This allows the wearer to increase the vertical tension in the web structure, which decreases the load placed on the knee. The semi-rigid structures and web framework are adjustable to offload force from the medial knee compartment. The web structure is also composed of silicone, which allows it to be flexible. Additionally, the thigh cuff and calf cuffs can be bent if heated to temperatures between 160-180 degrees Fahrenheit [42].

2.5.2 Tendon Compression Strap

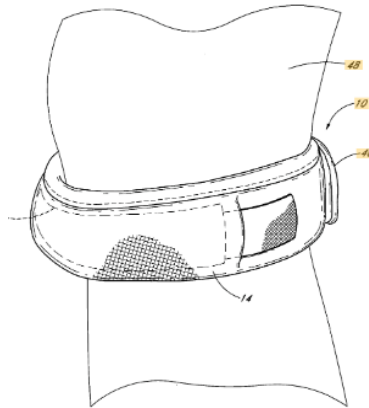


Figure 15. Tendon Compression Strap

(Source: <https://patents.google.com/patent/US20060069337A1/en?q=tendon&q=compressive&q=strap&oq=tendon>)

The tendon compressive strap patent claims to relieve anterior knee pain by applying pressure to the patella tendon at a position slightly above the tibial tuberosity. The main components of the brace, shown in Figure 15, include an adjustable strap and a compression member, made of a buttress inside a pouch. The patents claim that the buttress can be made of either elastic or inelastic material without compromising the effectiveness of the brace. The buttress also includes a bladder filled with small particles, such as small microspheres of glass, to provide further compression. The adjustable strap includes a hook and loop fastener for easy adjustment [43].

2.5.3 Air Brace

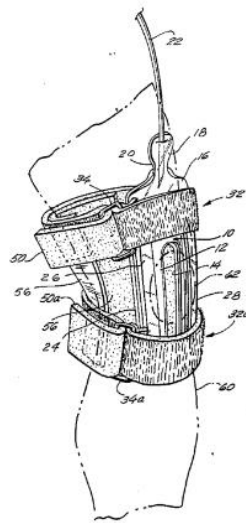


Figure 16. Adjustable Inflatable U-Shaped Air Cell Knee Brace

(Source: <https://patents.google.com/patent/US4872448A/en?q=patella&q=air&oq=patella>)

The Adjustable Inflatable U-Shaped Air Cell Knee Brace, shown in Figure 16, mainly focuses on realigning the patella and is best for patella malalignment and maltracking pain. By utilizing the U-shaped air pockets, pressure is applied to the affected areas of the knee. It claims to provide patella support without affecting the normal tracking movement of the leg [44]. There is an adjustable strap in order to provide a customizable fit around the region below the patella. This adjustability is important in allowing for a comfortable fit and ensuring that the brace will stay in the correct spot [44].

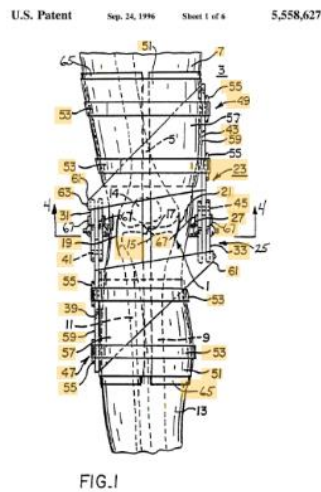


Figure 17. Front elevation view of the Orthopedic Brace with Inflatable Air Bag

(Source: <https://patents.google.com/patent/US5558627A/en?q=knee>)

The Orthopedic Brace with Inflatable Air Bag claims to support both sides of the knee to prevent injury to the patellofemoral joint. It has a hinged rigid support that is able to be locked at a certain angle to limit range of motion in order to prevent further injury. Additionally, the brace has a sensor attached to the side hinge. When the sensor detects potential for a high force, stress, strain or acceleration on the joint, the airbag is signaled to inflate to protect the joint [45]. The sensor has a programmable processor and allows for the user to set the threshold at which there will be a trigger signal to inflate the airbag. The brace also includes a pump for inflation of the air bag and a valve for deflation following the trigger signal [45].

3. Project Strategy

3.1 Initial Client Statement

The initial client statement was provided as follows: “Create a device that circumferentially pulls the patella away from the trochlea during the active flexion and extension of the knee, and is a gripping type of device for the patella hinged to the brace that avoids skin injury.” This statement was provided by the project’s sponsor, Doctor Robert Meislin, an orthopedic surgeon at New York University Langone Orthopedic Center, who specializes in general orthopedic surgery and orthopedic sports medicine. At Worcester Polytechnic Institute, Dr. Sakthikumar Ambady, a Biomedical Engineering Associate Teaching Professor, and Dr. Ahmet Can Sabuncu, a Mechanical Engineering Assistant Teaching Professor, advised this project.

3.2 Technical Design Requirements

Based on client specifications, industry standards, and team discussion, design objectives, constraints, and requirements were defined and are described in the following sections.

3.2.1 Design Objectives

Non-invasive: The design of the brace should be non-invasive, meaning that the brace cannot cut the skin or enter any part of the body. This is an important requirement, as a non-invasive approach is more suited to a larger population of patients and does not require any recovery time like an invasive approach would.

Relieve pain: One of the most important functions of the brace is to relieve patellofemoral pain. This can be quantified by evaluating the patient’s pain using Visual Analogue Scale (VAS), both before and after use of the brace. Patellofemoral pain is often evaluated on a 10 cm VAS, shown by Figure 18 [38]. The scale ranges from 0 (no pain) to 10 (worst pain possible) and is a reliable way for patients to rank the intensity of their pain.

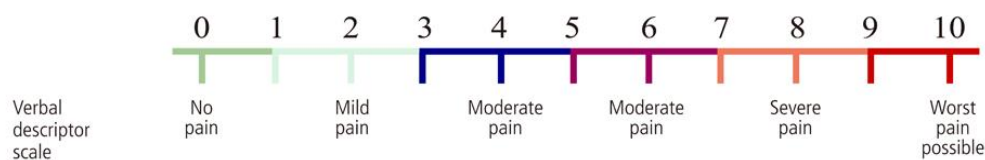


Figure 18. Visual Analogue Scale (VAS) for evaluating pain levels

(Source: <https://pubmed.ncbi.nlm.nih.gov/24327987/>)

Breathable: Since the brace is intended for exercise, it was important for the design to be breathable in order to resist sweat. A breathable fabric allows moisture to escape and not be trapped inside the brace. Breathability of fabric is measured in $\text{g/m}^2/24\text{hrs}$ and describes the amount of moisture vapor that can pass through each square meter of material in 24 hours. The higher the breathability, the better for exercise activities.

Reduce compression force on the patella: The key function of the brace was to be able to unload the patellar compression force that the patella is exerting on the femoral trochlea. Unloading this compression force reduces the patellofemoral forces and stresses acting on the joint. This helps alleviate the persistent pain experienced by the patients, as a result of these applied forces and stresses, in this anatomical region.

Adjustable: Adjustability was an essential component of an unloader knee brace because leg circumference and patellar geometry or dimensions vary from patient-to-patient. An unloader knee brace that is adjustable is more effective and comfortable than a brace that does not fit the patient properly. Adjustability increases the demand and market value of a brace since a variety of patients will be able to wear it in order to mitigate their patellofemoral pain. For example, a custom-design brace suitable for only one patient's anatomical specifications will have a higher cost than a universal, adjustable brace that is intended to be applicable for a greater range of patients in need of purchasing one to mitigate their patellofemoral pain.

Usable during physical activity: The brace was able to withstand repeated loading during physical activities such as walking, running, and jumping. The brace allows the knee joint to flex and extend naturally during activity which should also allow for the rotational moment (tibial torsion) of the femoral-tibial articulation as well. The brace has a high level of comfort and is able to be donned and doffed with ease as to facilitate compliance by the subject to wear it consistently to obtain the benefit of wearing such a device.

3.2.2 Design Constraints

The designed product allows for a relatively normal range of motion for the knee, so as to not impede regular activities. For a healthy individual, the average range of posterior knee flexion is about 139 degrees during passive weight-bearing movement and 135 degrees during active weight-bearing movement [46]. The minimum range of motion for the joint is 109 degrees during passive weight-bearing movement and 110 degrees during active weight-bearing movement [46]. The brace must maintain at least 75% of this minimum range of motion. Additionally, the knee brace does not cause skin irritation for

the patient. This design constraint was important since patients will not want to wear a brace that causes any additional pain or irritation. Along with this, the brace can be worn for an extended period of time without excessive discomfort. The patient should feel comfortable wearing the brace during all types of activity without annoyance.

The patellofemoral joint experiences a force of 4.3 to 7.9 times the body weight during running [47]. The average weight of a male between ages 20 and 39 is 196.9 pounds [48]. Since women weigh less on average, the male weight will be used to determine the design constraint. There are 4.45 N in one pound, which indicates that the brace must withstand 6,922 N (calculated according to the average male weight who experiences a knee force that is 7.9 times his body weight). Depending on the training regime, individuals might run between 30 and 40 miles per week if they are avid runners training for a long-distance race [49]. During a one-mile run, an individual takes between 1,000 and 2,000 steps [50]. If an individual runs 40 miles every week for an entire year, the brace must withstand 4.16 million loads. To make this brace last 3 years, which is the expected lifetime of a knee brace, it must withstand 12.5 million loadings [51].

In addition to product constraints, there are also time and budget constraints that had to be accounted for. The team had approximately 30 weeks from the beginning of the academic year to complete the project. Completion of the project was defined as successfully designing and building a prototype, testing it, and finishing the final report. The initial 8 weeks of this time period was dedicated to report writing and design brainstorming, while the remaining time was spent on design building and testing. Each team member was provided with \$250 for this project, accumulating in a total of \$1,250 for the team's final budget.

3.2.3 Design Operation and Components

The patellofemoral brace includes components that allow it to be attached to the thigh and shank to absorb the applied forces experienced at this joint during activities of daily living. The base of the brace, which wraps around the user's leg, is secured with velcro and has elastic straps attached to it to ensure that the brace can be adjusted accordingly. This will not only allow for further adjustability, but also comfort during high-intensity activities. Additionally, the breathable materials will prevent excessive perspiration from being contained within the brace.

3.3 Standard and Regulatory Design Requirements

In addition to the project requirements, the unloader knee brace complies with the standards outlined by international and regulatory bodies, many of which are summarized below.

- American Society for Testing and Materials (ASTM):

- *ASTM F2808, Standard Test Method for Performing Behind-the-Knee (BTK) Test for Evaluating Skin Irritation Response to Products and Materials That Come Into Repeated or Extended Contact with Skin*, describes procedures through which a material's potential for irritation of the skin over a long period of time is evaluated [52].
- *ASTM F2832, Standard Guide for Accelerated Corrosion Testing for Mechanical Fasteners*, outlines procedures for evaluating the ability of mechanical fasteners and their coatings to resist corrosion [53].
- *ASTM E6, Standard Terminology Relating to Methods of Mechanical Testing*, defines general terms related to mechanical testing [54].
- *ASTM E8/E8M, Standard Test Methods for Tension Testing of Metallic Materials*, describes tensile testing procedures for metallic materials [55].
- *ASTM D737, Standard Test Method for Air Permeability of Textile Fabrics*, outlines test methods for assessing a material's air permeability [56].
- US Food and Drug Administration (FDA):
 - *21 CFR 890.3475, Limb Orthoses*, defines orthotics and classifies similar products as Class I FDA devices. This regulation also exempts Class I devices from premarket notification requirements [57].
 - *21 CFR 890.5050, Daily activity assistive device*, defines daily activity assist devices and also exempts Class I devices from premarket notification requirements [58].
- International Organization for Standardization (ISO):
 - *ISO 22523:2006, External limb prostheses and external orthoses*, provides requirements and testing procedures for prostheses and orthoses [59].
 - *ISO 21063:2017, Prosthetics and orthotics*, describes the uses, functions, classifications and descriptions of soft orthoses [60].
 - *ISO 13404:2007, Prosthetics and orthotics*, categorizes and describes external orthoses and their components [61].
 - *ISO 854901:1989, Prosthetics and orthotics - Vocabulary - Part 1*, outlines terms describing external limb prostheses, orthoses, as well as the anatomical part of the body involved [62].
 - *ISO 8551:2003, Prosthetics and orthotics - Functional deficiencies*, describes the individual provided with an orthosis, clinical objectives of this treatment option, and its functional requirements [63].

The ASTM standard tests for skin irritation, material air permeability, and elasticity were something that the team needed to consider because the patellofemoral brace design has to meet requirements in these three areas. The FDA regulations simply state that the patellofemoral brace designed falls under Class I devices and therefore does not require premarket notification requirements, which is something the team will follow. Lastly, the team abided by the ISO standards outlined above to ensure that no additional tests needed to be performed on the brace and that the correct terminology was used to refer to the components of the final products.

3.4 Revised Client Statement

After gaining a better understanding of the various causes of patellofemoral pain from the literature review completed, it was necessary to revise the client statement to better fit the needs of a specific patient population. The revised client statement is as follows: "Create a device that reduces the patellar force on the trochlea during physical activity." The main problem being addressed is a lack of articular cartilage and malalignment of the knee joint, which leads to friction between the femur and the patella.

3.5 Management Approach

At the beginning of the project, the team outlined major project milestones and defined timelines for achieving them, represented by the project management Gantt Chart in Figure 19. The majority of the literature review and research was conducted in A-term, as well as several interviews of stakeholders and other resources. The team also defined project objectives and design functions, identified general project constraints, and developed a number of designs. At the end of the term, testing methods and procedures were researched and developed, and a final design was chosen. Materials were ordered and the initial design was constructed. The results from these tests were also analyzed, and final improvements were made to the design. Areas for future improvement were also identified during this term. In D-term, the team took time to complete the report and prepare a capstone presentation on the project. The project was submitted at the end of the academic year.

Category	Responsible Person	Task	Term	A-Term							B-Term							C-Term							D-Term						
			Week	1	2	3	4	5	6	7	1	2	3	4	5	6	7	1	2	3	4	5	6	7	1	2	3	4	5	6	7
Administrative	All	Meet with Advisors																													
	All	Write Report																													
	All	Develop Presentation																													
	All	Order Materials																													
Research	All	Literature Review																													
	All	Interview Stakeholders/ Other Sources																													
	All	Review of Current Solutions																													
	Caitlin, Ramona	Review of Standards and Regulations																													
	Jen, Mike, Megan	Review of Materials																													
Design Process	Ramona, Megan	Define Project Objectives																													
	Caitlin, Mike	Define Design Functions and Specifications																													
	Jen	Identify Project Constraints																													
	All	Develop Designs																													
	All	Identify Testing Equipment and Methods																													
	All	Develop Testing Procedures and Criteria																													
	All	Finalize Design																													
	All	Identify Materials																													
	All	Construct Brace																													
Product Testing, Evaluation, and Improvement	Caitlin, Mike, Ramona	Mechanical Testing of Brace I																													
	Megan, Jen	Human Testing of Brace I																													
	All	Evaluation of Test Results I																													
	All	Make Improvements																													
	Caitlin, Mike, Ramona	Mechanical Testing of Brace II																													
	Megan, Jen	Human Testing of Brace II																													
	All	Evaluation of Test Results II																													
	All	Make Improvements II																													
	All	Finalize Design																													
	All	Identify Areas of Future Improvement																													

Figure 19. Gantt Chart for tracking project progress

4. Design Process

4.1 Needs Analysis

Based on the literature review and interviews with key stakeholders such as athletic trainers and the target patient population, the team established minimum requirements the final product should meet. The patellofemoral unloader brace must be non-invasive and allow a range of motion that is at least 75% of minimum knee flexion (110 degrees) [46]. The product also needs to withstand 6,922 N of force placed on the knee and be able to reduce this force so that the level of pain reported by the wearer is reduced by at least one grade (according to the Visual Analogue Scale). To ensure durability, the brace must withstand 12.5 million loadings (based on a 3-year lifetime). In terms of comfortability on the skin, the brace must not cause skin irritation. Wearers should also report a grade of 0 on the VAS, which corresponds to “no pain”, when describing the comfort and fit of the brace. Furthermore, the brace must be breathable in nature, so that while engaging in physical activities, the brace does not retain moisture such as sweat and cause it to smell. To account for high perspiration due to high activity levels and weather conditions, the brace material must have a breathability of at least 9,000 g/m²/day [64].

Table 2. Pairwise Analysis Chart for ranking project objectives

Objectives	Non-invasive	Relieves pain	Low-cost	Adjustable	Usable during physical activity
Non-invasive		0	0	0	0
Relieves pain	1		0	0	0
Low-cost	1	1		0	0
Adjustable	1	1	1		0
Usable during physical activity	1	1	1	1	
Total	4	3	2	1	0

To rank the design objectives against each other based on the client’s needs and the project’s criteria, the team created a Pairwise Analysis Chart, shown by Table 2. The purpose of a Pairwise Analysis Chart is to organize and define the significance of each objective in the scope of the final design. A “1” in the cell indicates that the vertical objective was deemed more important than the horizontal objective, and a “0” in the cell indicates that the horizontal objective was deemed to be more important

than the vertical objective. That being said, objectives with low or null scores are not considered to be non-important; they are simply less critical than those with a higher score.

Using this scoring system, it was found that the two most critical objectives were that the design be non-invasive and relieve pain. The initial project statement provided by the client emphasized these two objectives and are essential parts of the design's function. The least significant objective was found to be the design's usability during physical activity. In comparison to all others, this had the least impact on the overall design function and was therefore less critical to add to the design.

In combination with the ranked objectives, the direction of the design was influenced by the design constraints listed in detail in Section 3.2.2. For example, the team needed to weigh the low cost of the materials and overall brace against the ability of the material to withstand the repeated loads from the user to determine whether to use a more expensive, more durable material, or a less expensive, less durable material.

4.2 Concept Maps

4.2.1 Initial Designs

Anti-Gravity Brace

One design for consideration was to use a spring and damper system in order to absorb some of the forces and take part of the impact off the knee. By using springs, the high forces on the knee would be surpassed and instead absorbed by the springs. Ideally, if the forces on the patella are dampened, then this would lead to less compressive forces and therefore less contact between patella and trochlear groove.

This design, shown in Figure 20, would be worn relatively higher on the thigh and would need to extend past just the knees, unlike most knee braces on the market. This could discourage people from wearing it because of the larger size. Another challenge with this design is the adjustability aspect. Since the brace would extend for almost half of the leg length, different heights and leg lengths would need to be considered. The brace would need to be able to adjust to the correct length, as a standard small, medium, or large sizing would not be specific enough to each person.

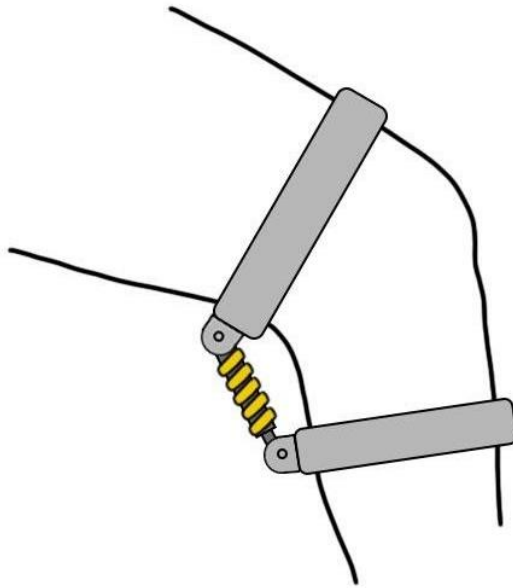


Figure 20. Anti-Gravity Brace Design

Inflation Pocket Brace with Pull-Over Strap

Within the patellofemoral joint, the patella tends to track laterally due to the greater pulling forces of the *vastus lateralis* and iliotibial band compared with the pulling force of the *vastus medialis*. This lateral tracking results in continuous contact between the posterior patella and anterior surface of the lateral femoral condyle, resulting in patellofemoral pain for the patient. A brace that will promote a medial tracking of the patella will mitigate the patellar compression resultant force that is caused by continuous surface contact of the posterior patella with the anterior lateral femoral condyle. Furthermore, reduced contact between the posterior patella and femoral trochlea will reduce the patellofemoral joint stress exerted on the joint, abating the degradation of the articular cartilage (known as osteoarthritis) on the posterior patella and will alleviate pain for the patient in this anatomical region.

This design, shown in Figure 21, incorporates two small inflatable air pockets: one positioned on the lateral side of the patella and the other positioned on the superior side of the patella. The desired purpose of these air pockets is to induce proper medial inferior tracking of the patella within the patellofemoral joint. To account for varying patellar dimensions from patient to patient, the brace will possess an elastic hole to improve the grip on the patella, thus improving the air pockets' efficacy in deviating the patella medially and inferiorly. Additionally, the brace will also possess a pull-over strap, with an elastic hole matching the size of the hole on the brace, in order to compress (applying more pressure to) the air pockets resulting in an augmented medial, inferior pulling force on the patella.

The key advantage of this design is that the size of the air pockets can be adjusted in order to sufficiently grip the patella, depending on the patient's patellar dimensions, to promote proper patellar

tracking. The air pockets will have small ports where an external pump or pressure cuff can connect to inflate or deflate the air pockets. The brace will be fabricated with breathable, and flexible neoprene material that will be comfortable for patients with a variety of leg circumferences and patellar dimensions.

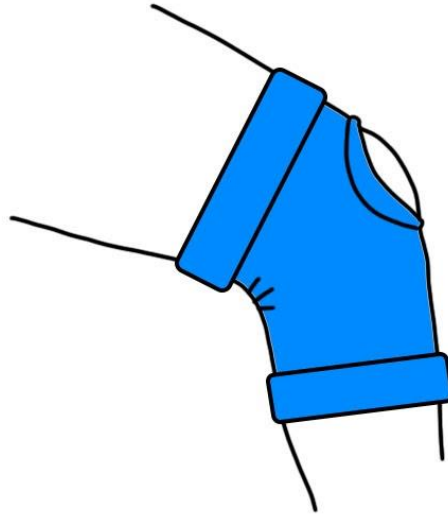


Figure 21. Inflation Pocket Brace with Pullover Strap Design

Shock Absorbing Brace

Another preliminary design was to incorporate a shock absorbing material into the brace. Similar to the anti-gravity brace concept, this design would absorb some of the forces caused by impact activities using the collision of shock absorbing materials, such as polyurethane. During activity, discs or rings made of shock absorbing material wrapped around a movable telescopic rod would move towards each other in the flexion stage of motion. As the discs collide with one another and compress, a percentage of the impact forces would be dissipated between the knee and the discs, resulting in a lower overall shock through the knee.

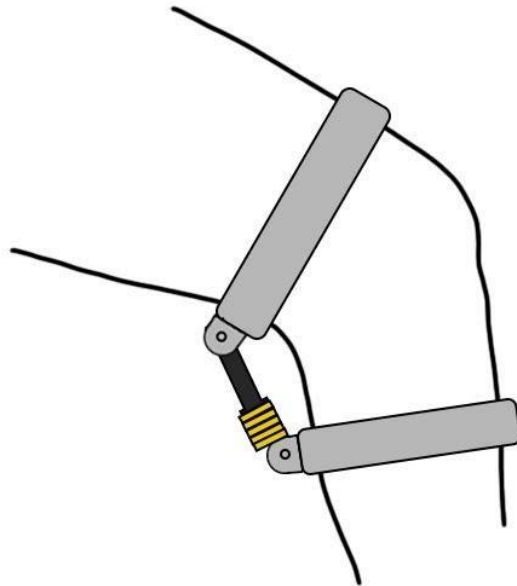


Figure 22. Shock Absorbing Brace Design

The benefit of this design is that the telescopic rod can allow for a large range of flexion without inhibiting overall mobility of the wearer. This design also does not encourage muscle atrophy, enabling the wearer to utilize the full strength of their muscles. Furthermore, there are many shock absorbing materials available on the market, allowing for tailorable properties.

4.2.2 Preliminary Design Analysis

To ensure that the development of the product was feasible, the team focused on several design aspects. The first focused on the financial feasibility of the design. With a limited budget and the requirement to create a low-cost product, the materials and equipment needed to create the brace were chosen carefully. In order to test the feasibility of the final design, the team researched the materials needed to build the brace and compared the cost to that of current knee braces on the market. Additionally, equipment needed to build the device or testing materials that the team purchased with the budget was taken into consideration. Similarly, the feasibility of testing the device was also considered regarding testing equipment, test subjects, and time constraints. To determine the efficiency of the knee brace in reducing the patellofemoral compression force, the forces on the patellofemoral joint were analyzed. The final product was also tested on subjects to determine its comfortability. However, due to the limited time available to complete the entirety of this project, the team carefully planned and followed a strict testing schedule. Lastly, the technical knowledge was further considered as well. The team was

composed of individuals who have biomedical engineering and mechanical engineering backgrounds. It was important that the team did not delve into areas that were completely outside the scope of their capabilities, since doing so would have prevented the successful completion of this project.

Given the need to reduce the compressive force on the patellofemoral joint, the inflation pocket brace with a pullover strap was no longer considered as one of the team’s final designs, since this brace was intended to realign the patella to ensure that it is not offset in the trochlear groove. While patella alignment can help reduce patellofemoral pain as well, it does not directly prevent the friction between the tibia and the patella. This patella realignment brace therefore is missing the component that could reduce this friction, which is why the team decided to choose the shock absorbing brace and the anti-gravity brace as the final designs to be compared.

4.2.3 Final Design Analysis

Final Design Selection

Ultimately, the team decided to alleviate patellofemoral pain by reducing the compression forces at the knee, rather than realigning or anteriorly translating the patella. The two remaining designs were the anti-gravity and shock absorbing braces, which were then compared in the Pugh Analysis in Table 3.

Table 3. Pugh Analysis chart for final design selection

Criteria	Weight Factor	Current Solution	Alternative Solutions	
		Reaction Web Brace	Anti-Gravity Brace	Shock Absorption Brace
Ease of static extension	4	0	-1	0
Ease of static compression	4	0	-1	-1
Lightweight	3	0	-1	-1
Cost-effective	2	0	-1	0
Time to implement	2	0	-1	0
Adjustable	3	0	0	1
Ability to reduce force	5	0	1	1
Wearer comfort	4	0	-1	1
Durable	3	0	0	1
Total		0	-14	8

The Pugh Analysis lists the criteria of the final design, which are ranked on a scale from 1-5 in order of importance. A weight of 5 indicates that the criteria is most important and should be prioritized

when designing the product. The alternative solutions listed are compared to a gold standard, the reaction web brace that is currently available on the market to help reduce patellofemoral pain. The criteria of the current solution are all given a score of 0. The alternatives are ranked with a score of “1” or “-1”. A score of “1” indicates that the alternative design can meet the respective criterion better than the current solution. A score of “-1” indicates that the alternative design cannot meet the criterion as well as the current solution. A score of “0” indicates that there is little to no difference between the alternative design and current solution regarding the respective criterion. For each alternative solution, the scores given for each criterion are summed up. As illustrated in the table above, the spring damper brace obtained a score of -16, while the shock absorption brace obtained a score of 6, indicating the ability of the latter design to achieve the necessary design criteria.

Materials Selection

The cuffs of the brace, highlighted in Figure 23, are made of hardened, easy-to-form pure aluminum 1100 sheets. Pure aluminum is resistant to corrosion, which is necessary for a brace that is intended to be used during physical exercise and will be subjected to perspiration. Pure aluminum 1100 is also flexible enough to bend, light, yet strong enough to hold its desired shape without deforming [65]. To prevent the metal cuffs from being in direct contact with the skin, the cuffs will be covered in neoprene, which is a synthetic rubber often used in knee braces. Neoprene is weather, water, and tear resistant, making it suitable for outdoor applications. The material is also smooth and soft, so it will ensure that the individual wearing the brace does not feel the metal cuffs and that no perspiration is trapped in the neoprene sleeve around the aluminum cuffs. Being water resistant, the brace will also prevent unpleasant odors [66].

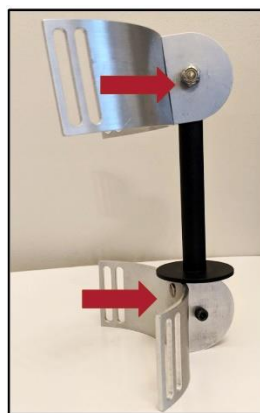


Figure 23. Cuff component of brace prototype

The telescopic rod, highlighted in Figure 24, lined with an absorbing material is the second element of the knee brace. The shock absorbing material, highlighted in Figure 25, is nitrile rubber (NBR) foam, a synthetic rubber copolymer that has a high damping coefficient, making it efficient in absorbing

shock for millions of cycles. The telescopic rod will be composed of impact-resistant polycarbonate. This polycarbonate is easily machinable, light and strong, so it can reduce the overall weight of the brace but still be able to withstand the forces placed on it [67]. The telescopic rod will be attached to the aluminum cuffs with pin joints. The pin joint attachments will be composed of stainless steel and the pins will be made of 416 stainless steel, which offers a high breaking strength [68].

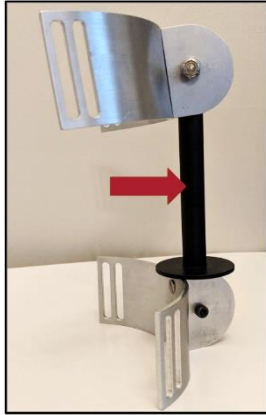


Figure 24. Telescopic rod component of brace prototype



Figure 25. NBR component of brace prototype

4.3 Design Calculations and Modeling

In order to evaluate if the design for a shock absorbing brace would have a significant impact on the force reduction at the knee joint, hand calculations were done, and models were created. The main parameters to be calculated were the joint reaction forces and the force that the brace exerts on the leg. For these calculations to be made, first a schematic must be drawn with a reference frame to visualize the aspects of the analysis. Figures 26 and 27 show schematics of the leg without and with the brace, respectively. Figures 28 and 29 show the consolidated quadriceps and patellar forces.

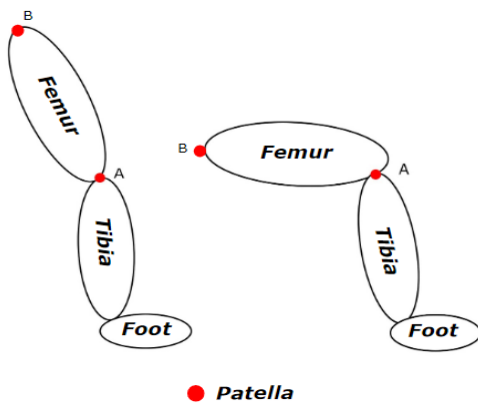


Figure 26. Leg schematic without brace

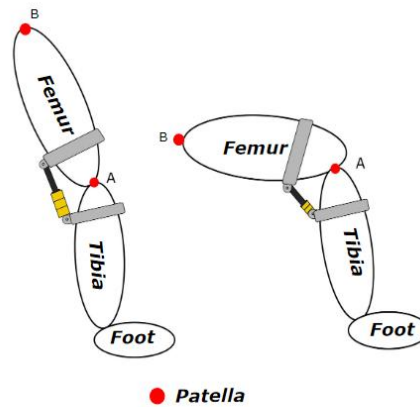


Figure 27. Leg schematic with brace

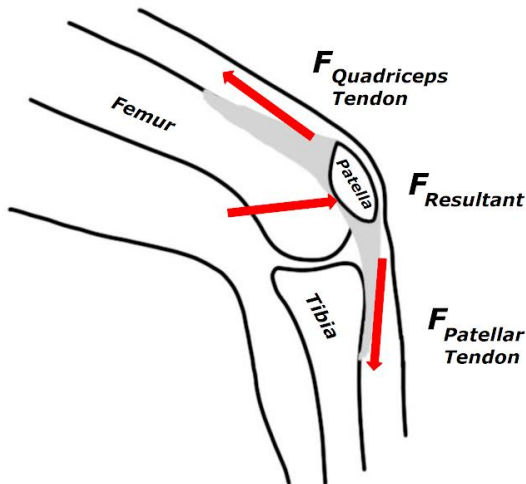


Figure 28. Patellar forces without brace

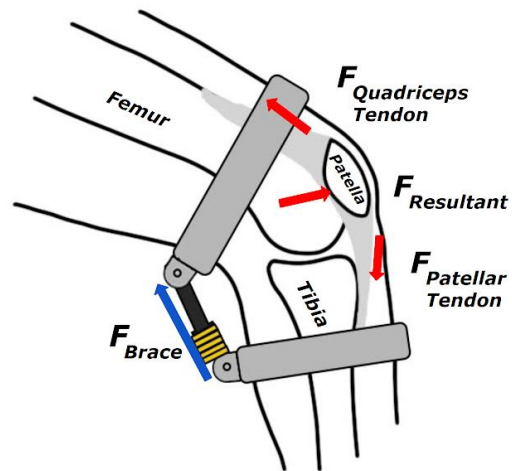


Figure 29. Patellar forces with brace

To analyze the force on the knee joint, the following assumptions were made for the preliminary analysis in reference to Figures 26-29:

1. The person is 5'6" and 140 pounds (approximately 1.67 meters and 64 kilograms).
2. The force on the knee is directed at an angle of 30° from the femur.
3. This is a static scenario (e.g., the person is holding a squat).
4. The angle between the femur and the tibia is 90° when fully flexed.
5. The length of the person's thigh is 42.2 cm, r_{TH} .
6. The weight of the upper body is directed at the hip (point B).
7. The rod is directed at an angle of 45° and is 22.5 cm from the patella (point A) on the femur.
8. In Figures 28 and 29, $F_{Resultant}$ is a consolidation of $F_{Quadriceps Tendon}$ and $F_{Patellar Tendon}$.

Before calculations can be done to find the joint forces at the knee, calculations must be done to find the weight of the thigh, center of mass of the thigh, and the weight of the upper body. These calculations are done by using anthropometric data [69]. Figure 30 below shows the free body diagram for the thigh without the brace with all relevant forces acting on it with the above assumptions, with F_{WUB} representing the force from the weight of the upper body, F_{WT} representing the force from the weight of the thigh, and $F_{Patella}$ representing the force on patella exerted by the quadriceps and patellar tendons.

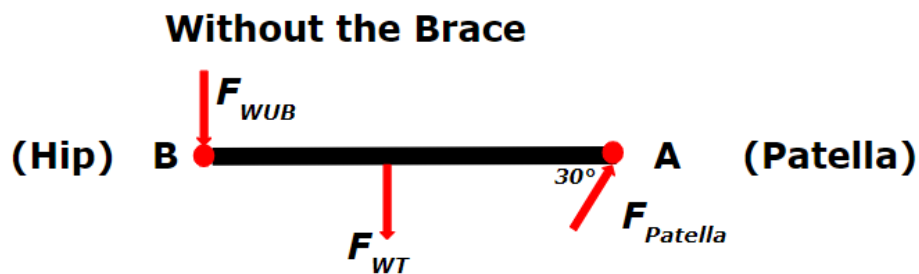


Figure 30. Free body diagram without brace during knee flexion

From the free body diagram in Figure 30, Equation 1 can be used to evaluate the force on the patella in the y-direction, $F_{Patella}$, when there is no brace on the leg.

$$\begin{aligned}\sum F_y &= -F_{WUB} - F_{WT} + F_{Patella}(\sin 30^\circ) = 0 \\ 0 &= -425.55 \text{ N} - 62.76 \text{ N} + F_{Patella}(\sin 30^\circ) \\ F_{Patella} &= (488.31 \text{ N}) \div (\sin 30^\circ) \\ F_{Patella} &= 977 \text{ N}\end{aligned}\tag{1}$$

Figure 31 below shows the free body diagram for the thigh with the brace with all relevant forces acting on it. The same assumptions above apply, as well as the same defined variables with the addition of F_{BR} representing the force of the brace. F_{BR} is assumed to be acting at an angle of 45° .

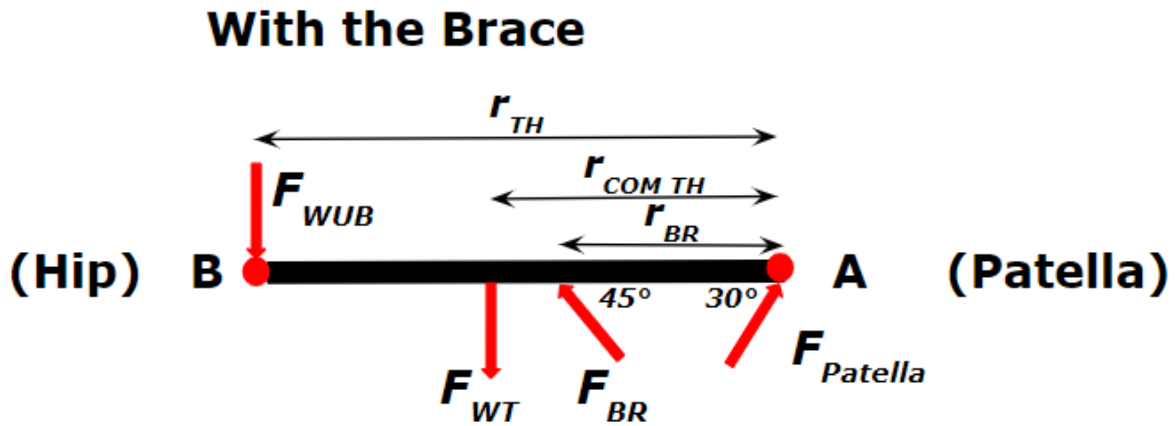


Figure 31. Free body diagram with brace during knee flexion

The following equations were used to evaluate the force on the patella, $F_{Patella}$ with the brace on the leg. Equation 2 sums the forces in the y-direction to obtain the force of the brace, F_{BR} . This value is then used in Equation 3, which takes the sum of the moments around point A to find the force on the patella, $F_{Patella}$.

$$\sum F_y = -F_{WUB} - F_{WT} + F_{BR}(\sin 45^\circ) + F_{Patella}(\sin 30^\circ) = 0\tag{2}$$

$$F_{BR} = [(F_{WUB} + F_{WT} - F_{Patella}(\sin 30^\circ))] \div (\sin 45^\circ)$$

$$F_{BR} = (488.31 \text{ N} - F_{Patella}(\sin 30^\circ)) \div (\sin 45^\circ)\tag{3}$$

$$\sum M_A = M_{WUB} + M_{WT} - M_{Bry} = 0\tag{4}$$

$$0 = (r_{TH} \times F_{WUB}) + (r_{COM(thigh)} \times F_{WT}) - (r_{BR} \times F_{BR} (\sin 45^\circ))$$

$$0 = (0.422 \text{ m})(425.55 \text{ N}) + (0.24 \text{ m})(62.76 \text{ N}) - r_{BR}(488.31 \text{ N} - F_{Patella}(\sin 30^\circ))$$

$$0 = 194.58 \text{ N}\cdot\text{m} - 0.225 \text{ m}(488.31 - F_{Patella}(\sin 30^\circ))$$

$$0 = 194.58 \text{ N}\cdot\text{m} - 109.87 \text{ N}\cdot\text{m} + 0.225(F_{Patella}(\sin 30^\circ))$$

$$0 = 84.71 \text{ N}\cdot\text{m} + 0.11(F_{Patella})$$

$$F_{Patella} = -753 \text{ N}$$

The above equations are included in Appendix A with more detail and full calculations. The values obtained with these equations were used to evaluate the estimated force that the brace will have on the leg and the forces that the patella experiences that the brace is looking to counteract. These equations will be used for reference after testing is conducted to validate the effectiveness of the shock absorbing brace. The reason why F_{Patella} is negative is due to the counteracting force from the brace that is now present. The brace is providing more support than what the initial F_{Patella} load was. This is only the case in this static scenario when the brace is used in real-world applications. Nonetheless, regarding magnitude, the F_{Patella} decreases when the brace is introduced, which was expected.

Design Optimization

The team performed preliminary design optimization tests to determine the design specifications and parameters that would achieve both maximum shock absorption and comfort for the wearer. First, theoretical calculations were done to find the distance between the cuff and the distal end of the thigh that would offer maximum support. This optimal distance, r_{BR} , shown in Figure 32, is specifically defined as the length between circumferential midline of the thigh cuff and the popliteal fossa, the shallow groove located on the posterior knee.

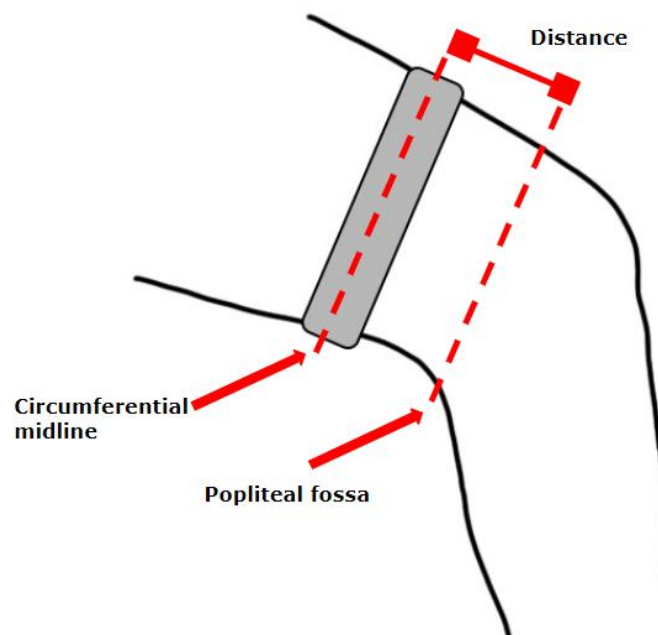


Figure 32. Diagram showing the distance measurement

Modifying the calculations used above, the team was able to derive an equation to determine the force supported by the brace, F_{BR} , at varied distances, r_{BR} .

$$\sum F_y = -F_{WUB} - F_{WT} + F_{BR}(\sin 45^\circ) + F_{Patella}(\sin 30^\circ) = 0 \quad (2)$$

Equation 2 was rearranged to solve for F_{BR} as shown below.

$$\begin{aligned} F_{BR} &= [(F_{WUB} + F_{WT} - F_{Patella}(\sin 30^\circ))] \div (\sin 45^\circ) \\ F_{BR} &= (488.31 \text{ N} - F_{Patella}(\sin 30^\circ)) \div (\sin 45^\circ) \end{aligned} \quad (3)$$

Equation 3 was substituted for F_{BR} into Equation 4 below.

$$\begin{aligned} \sum M_A &= M_{WUB} + M_{WT} - M_{Bry} = 0 \quad (4) \\ 0 &= (r_{TH} \times F_{WUB}) + (r_{COM}(\text{thigh}) \times F_{WT}) - (r_{BR} \times F_{BR}(\sin 45^\circ)) \\ 0 &= (0.422 \text{ m})(425.55 \text{ N}) + (0.24 \text{ m})(62.76 \text{ N}) - r_{BR}(488.31 \text{ N} - F_{Patella}(\sin 30^\circ)) \\ 194.58 \text{ N}\cdot\text{m} &= r_{BR}(488.31 - F_{Patella}(\sin 30^\circ)) \\ F_{Patella} &= -[(194.58 \div r_{BR}) - 488.31] \div (\sin 30^\circ) \end{aligned}$$

In Table 4, the team designated the highlighted cells as the most optimal distances between the cuff and the knee in order to decrease $F_{Patella}$. While distances of less than 0.2 meters theoretically yielded greater amounts of force supported by the brace, it was determined that if the cuff be placed too close to the knee, the wearer may experience a greater level of discomfort due to an increased torque caused by the supportive force. Distances greater than 0.275 meters were also excluded from the optimal range due to the decreased supportive force. The force that is supported by the brace was also included in the table. As mentioned above, the force supported by the brace, F_{BR} , is greater than the force on the patella when the distance from the knee joint is greater than 0.2 meters, which is why the $F_{Patella}$ appears to be negative.

Table 4. Distance optimization data

Distance from knee joint		$F_{Patella}$	F_{BR}
inches	meters	(Newtons)	(Newtons)
0.984	0.025	-14589.916	7783.958
1.969	0.050	-6806.648	3892.324
2.953	0.075	-4212.225	2595.113
3.937	0.100	-2915.014	2595.113
4.921	0.125	-2136.687	1297.901
5.906	0.150	-1617.803	1297.901
6.890	0.175	-1247.171	1112.585
7.874	0.200	-969.197	973.599
8.858	0.225	-752.995	865.498
9.843	0.250	-580.034	779.017
10.827	0.275	-438.520	708.260
11.811	0.300	-320.591	649.296
12.795	0.325	-220.806	599.403
13.780	0.350	-135.275	556.638
14.764	0.375	-61.149	519.575

5. Design Verification

5.1 Methodology Summary

5.1.1 Skin Electromyography (EMG) Protocol

Electromyography, or EMG, is a test that can be performed in order to measure muscle response and electric activity in muscles. The EMG shows a measure of the nerve's stimulation in the muscle, and detects the muscle activation through different movements and conditions. EMGs can be done through either intrusive or non-intrusive techniques. For the purpose of this project, a skin EMG was performed with electrodes placed on the surface of the skin. The EMG signal can be exported into a comprehensive graph that tracks the membrane potential of the muscle signals over time. The resting potential of the muscle fibers are approximately -80 to -90 mV when the muscles are not in contraction, and the action potential will bring the membrane potential to approximately +30 mV due to the influx of Na^+ through its depolarization. The signal will then repolarize, hyperpolarize below the resting potential, and then hit its resting potential again.

The skin EMG test will be used to compare the muscle activation during motion (running, squats, stairs and lunges) with the shock absorbing brace, without a brace and with the DonJoy Reaction Web Brace. In order to record the signal in the muscles of interest, two electrodes were placed on the *rectus femoris*, *vastus lateralis* and *vastus medialis* as seen in Figures 33 and 34.

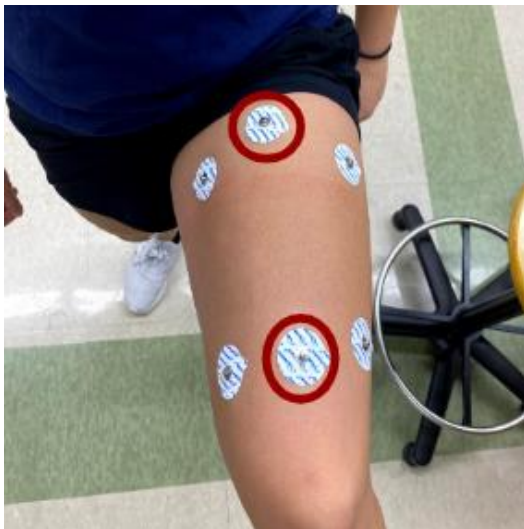


Figure 33. Example placement of electrodes on the *rectus femoris* (circled)

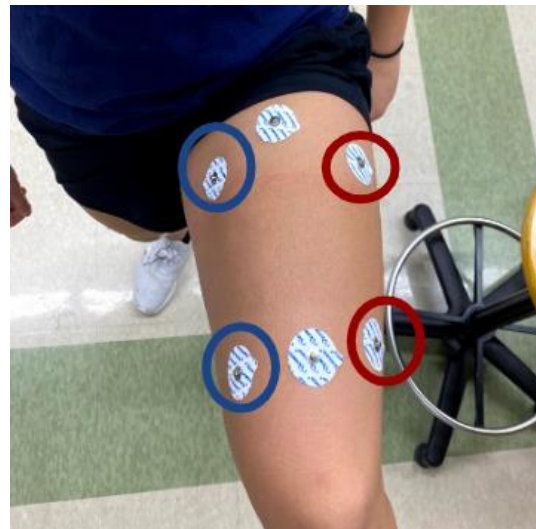


Figure 34. Example placement of electrodes on the *vastus medialis* (circled in blue) and *lateralis* (circled in red)

With use of our brace, the muscle activity of the vastus lateralis, vastus medialis and rectus femoris should decrease since the force at the knee joint will be distributed to the shock absorbing portion

of the brace, thereby decreasing the activity of these leg muscles. The voltage outputs will be compared to show if a reduction of force on the knee was present. A detailed protocol for the skin EMG test can be found in Appendix B of this report and results of the testing procedures can be found in subsequent sections.

5.1.2 Nitrile Rubber Force Reduction – Force Plate Protocol

To determine the amount of force that the knee brace can support, a force plate was used to determine the force of impact with and without the shock absorbing material. Varying weight was dropped onto the force plate when it was uncovered and covered with a nitrile rubber sheet. The number of nitrile rubber sheets was gradually increased to determine the amount of force that multiple layers can reduce. Ideally, the nitrile rubber would absorb some of the impact shock from the impact of the dropped weight and the force recorded by the force plate will be lower. The difference between the force recorded without the shock absorbing material and the force recorded with the shock absorbing material was calculated and results are found in subsequent sections.

A detailed protocol for the force reduction testing can be found in Appendix C of this report.

5.2 Summary of Data Collection and Analysis

5.2.1 Skin Electromyography Testing Results

5.2.1.1 Running

Three subjects participated in the running trials with our brace design, no brace and with the DonJoy Reaction Web Brace. An example of the experimental set-up is shown in Figure 35.



Figure 35. Example experimental setup for a treadmill run

Following the skin EMG testing, raw data from each of the trials was graphed. Figure 37 below shows examples of the raw data from trials during the no brace condition. According to literature, the maximum peaks seen in the *rectus femoris* raw data (shown in Figure 36) are during the toe off phase of the gait cycle [70]. The maximum peaks in the *vastus lateralis/medialis* raw data are during the heel off phase.

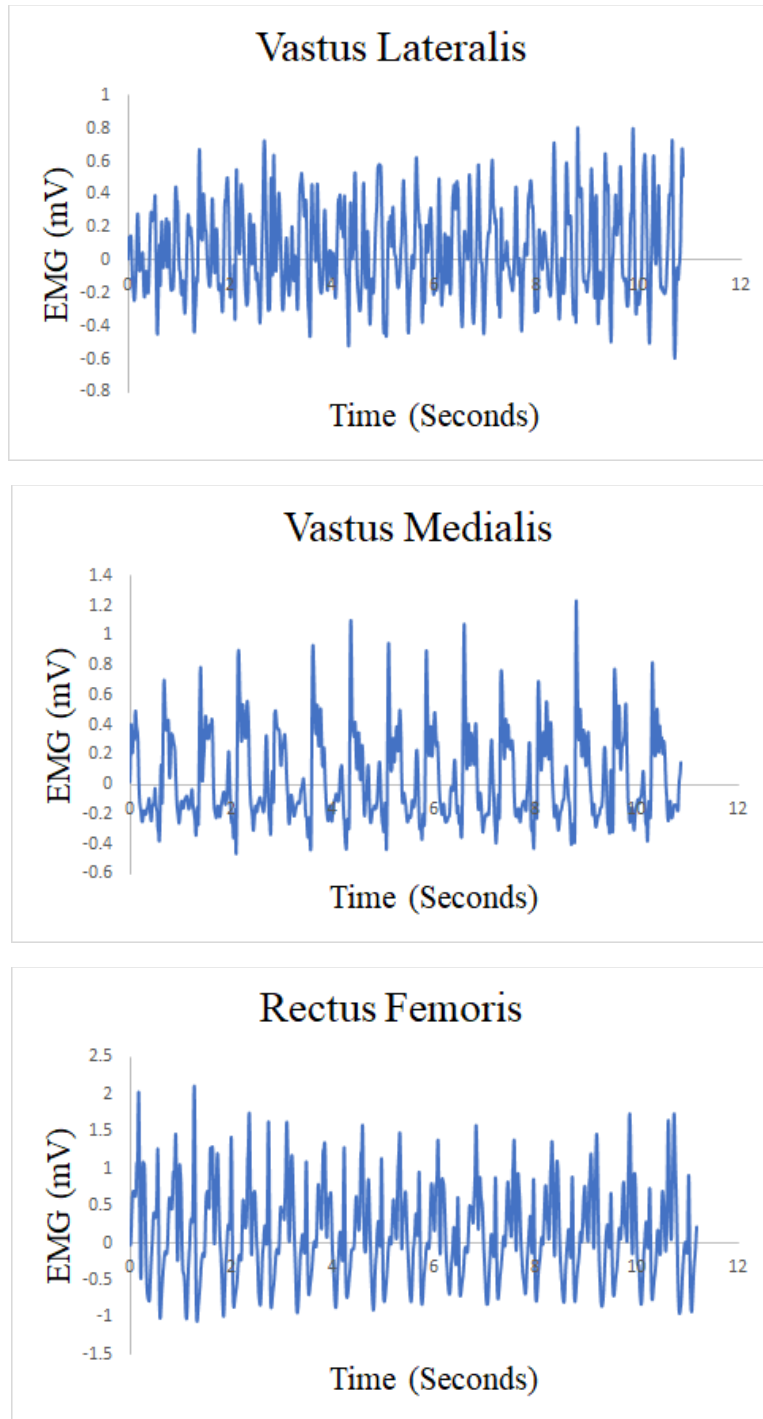


Figure 36. Example raw dominant leg EMG signal data during running

The raw data from each trial was run through a MATLAB script. For the data collected from the running trials, the MATLAB script calculated the local maxima of each data set. The maximas were then arranged in descending order and the first quarter of the maximas were used to calculate the average maximum peaks of each trial in each muscle. Outliers were removed prior to taking the average. A total average from the nine trials was calculated per condition. The total averages per condition can be seen in Table 5.

Table 5. Average maximum peaks of EMG signals during running.

Muscle group → Brace condition ↓	<i>Rectus Femoris</i> (mV)	<i>Vastus Lateralis</i> (mV)	<i>Vastus Medialis</i> (mV)
Our Brace Design	0.66	1.73	0.60
No Brace	0.91	0.93	0.75
DonJoy Reaction Web Brace	0.84	1.09	0.87

Figure 37 is shown below for an easy visual comparison between the three conditions.

Further analysis of these results can be found in Section 6.2.1.

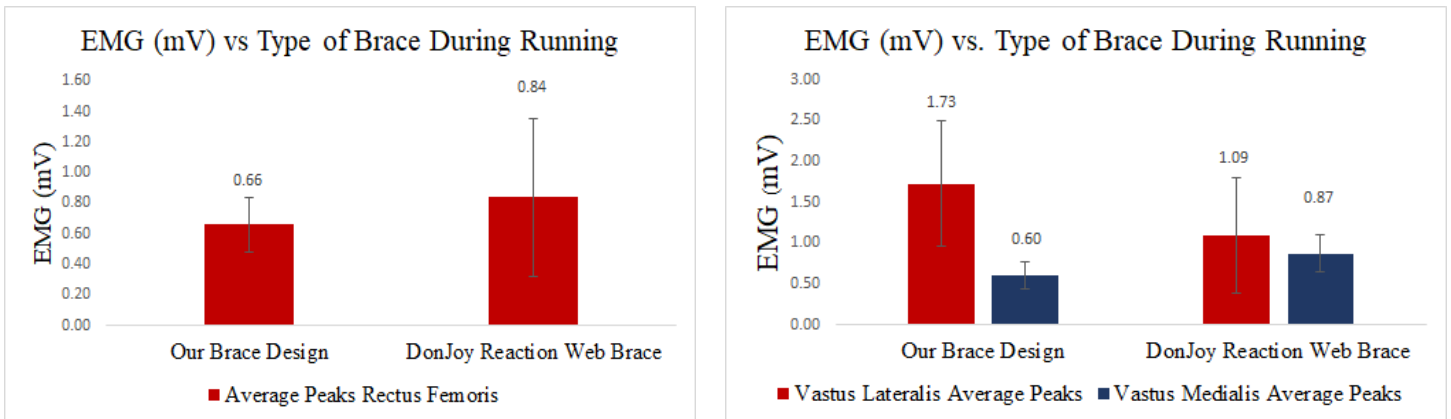


Figure 37. Total average maximum peaks of rectus femoris (left) and vastus medialis/lateralis (right) EMG signals during running.

5.2.1.1 Squats, Stairs, and Lunges

One subject participated in various exercises (squats, stairs, and lunges) with our brace design, no brace, and the DonJoy Reaction Web Brace. An example of the experimental set-up is shown in Figure 38.



Figure 38. Example experimental setup for a squat

The raw data that was collected from the skin EMG was graphed individually for each trial. An example of the raw data during one trial of squats is shown in Figure 39. Maximum peaks in *vastus medialis* and *vastus lateralis* during squats are typically seen in the initial ascent, which is about 45-68 degrees of knee flexion. For the *rectus femoris*, maximum activity is typically seen in the final descent (about 23-45 degrees of knee flexion) [71].

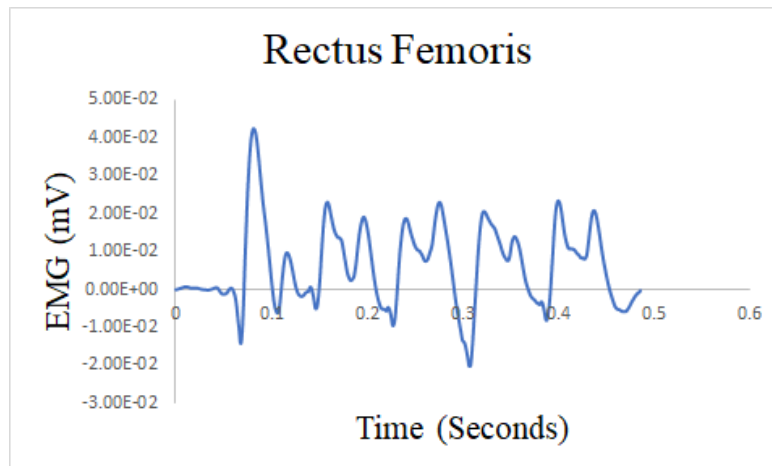
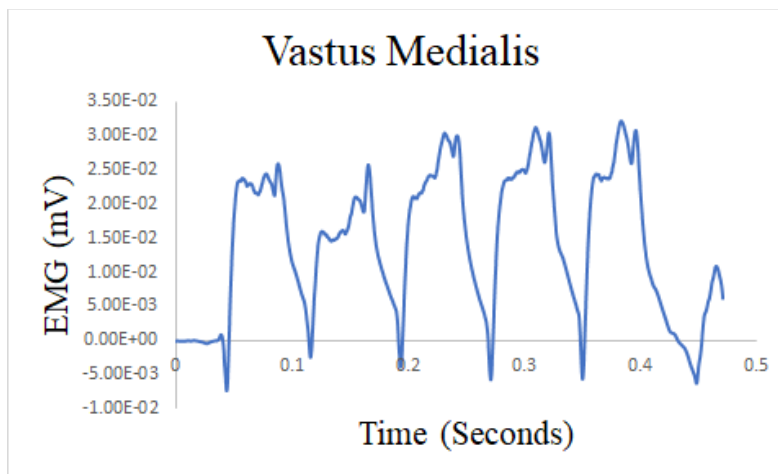
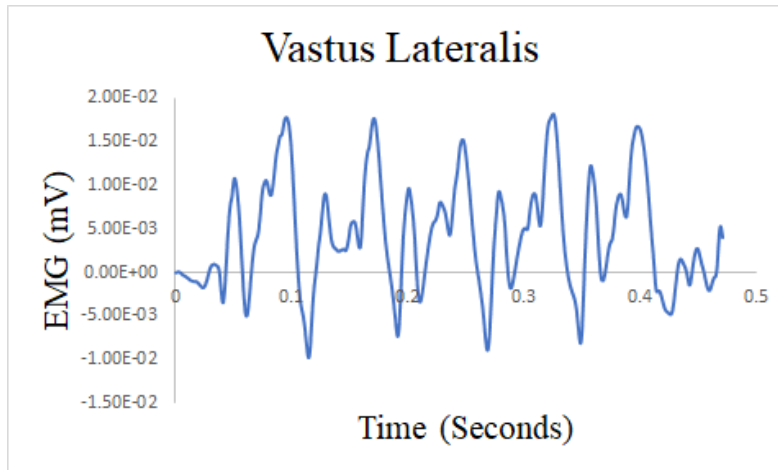


Figure 39. Example raw dominant leg EMG signal data during squats

After the raw data was collected, it was run through a MATLAB script to find the maximum peaks. The top five maximum peaks were calculated, and outliers were removed. A total maximum average was calculated per each muscle, activity, and condition. The results of these total averages are

displayed in Tables 6-8 below. Data for *rectus femoris* signals during lunges was not recorded due to limitations from COVID-19.

Table 6. Average maximum peaks of EMG signal during squats

Muscle group → Brace condition ↓	Rectus Femoris (mV)	Vastus Lateralis (mV)	Vastus Medialis (mV)
Our Brace Design	0.05	0.02	0.03
No Brace	0.03	0.03	0.03
DonJoy Reaction Web Brace	0.29	0.32	0.46

Table 7. Average maximum peaks of EMG signal during stairs

Muscle group → Brace condition ↓	Rectus Femoris (mV)	Vastus Lateralis (mV)	Vastus Medialis (mV)
Our Brace Design	0.02	0.01	0.02
No Brace	0.02	0.02	0.02
DonJoy Reaction Web Brace	0.43	0.64	0.51

Table 8. Average maximum peaks of EMG signal during lunges

Muscle group → Brace condition ↓	Rectus Femoris (mV)	Vastus Lateralis (mV)	Vastus Medialis (mV)
Our Brace Design	0.03	0.02	--
No Brace	0.03	0.02	--
DonJoy Reaction Web Brace	0.46	0.51	--

Figure 40 below shows the data in Tables 6-8 in graphical form for an easier visual. *Vastus lateralis* and *vastus medialis* are shown on the same graphs for a direct comparison between the two muscles under the same conditions. Further analysis of these results can be found in Section 6.2.1.



Figure 40. A collection of graphs that show average maximum peak data during various activities.

5.2.2 Force Plate Testing Results

After conducting the force plate testing, a graph that compares the force collected at each data point was generated by the software used. The data points are in chronological order, helping them illustrate the time frame of the experiment. An example of such a graph is included below; this graph belongs to one of the trials in which the 5-pound weight was dropped on the uncovered force plate five times.

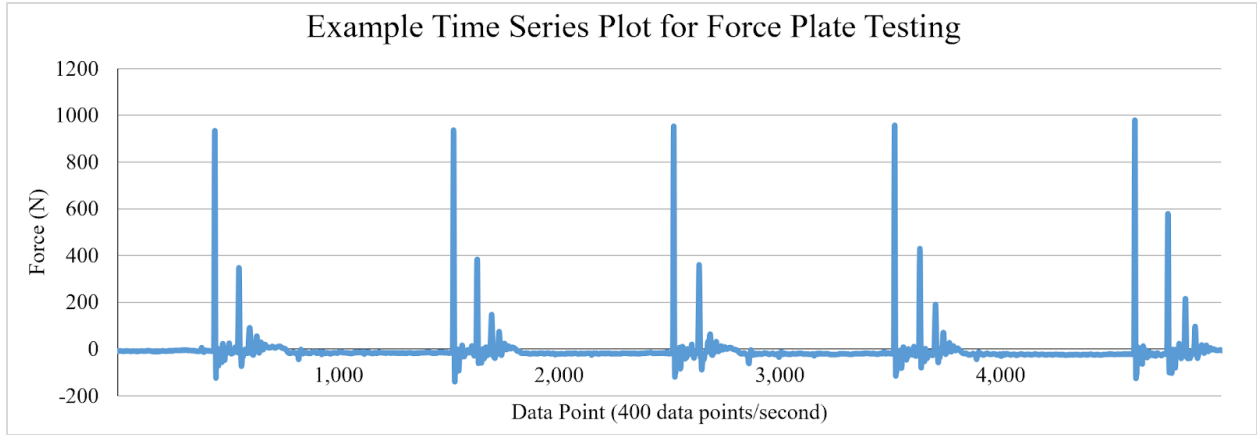


Figure 41. Vertical impact force values using a 5-lb weight versus time

The highest peaks recorded illustrate the force when the weight hit the force plate the first time, which therefore indicates its impact force. These impact forces were translated into the force graphs shown below which compare the impact force with the number of layers of NBR.

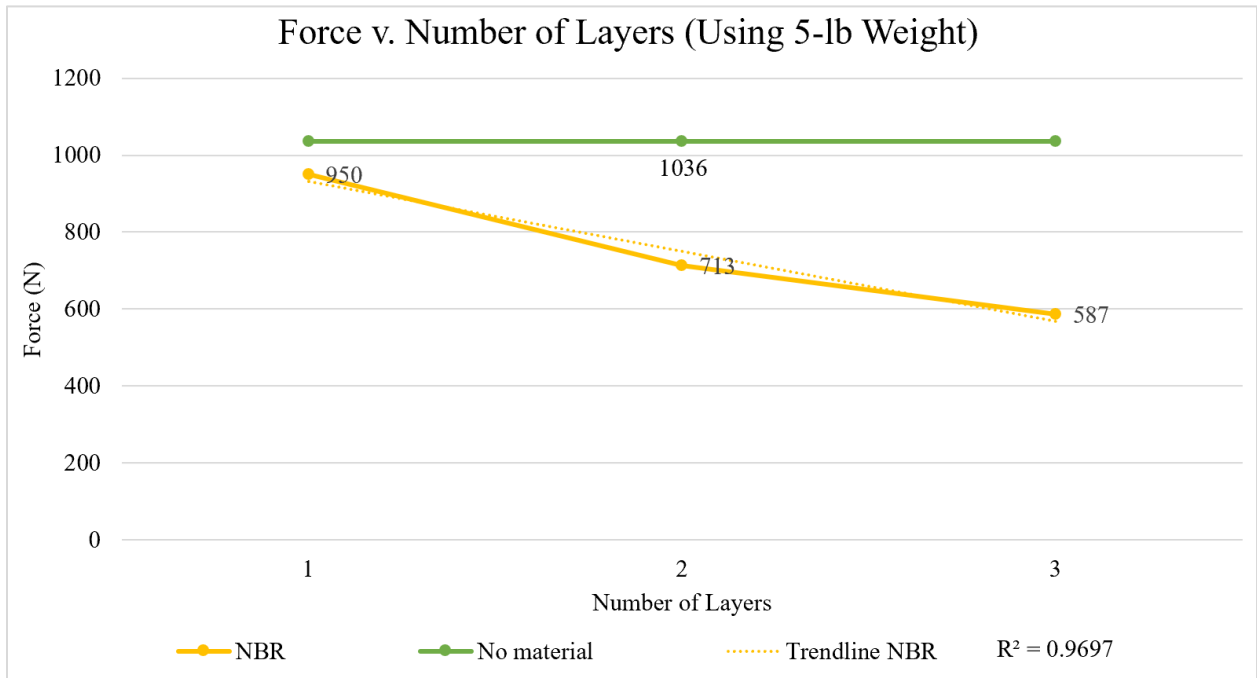


Figure 42. Measured vertical impact force values (N) from NBR and no material test conditions using a 5-lb weight

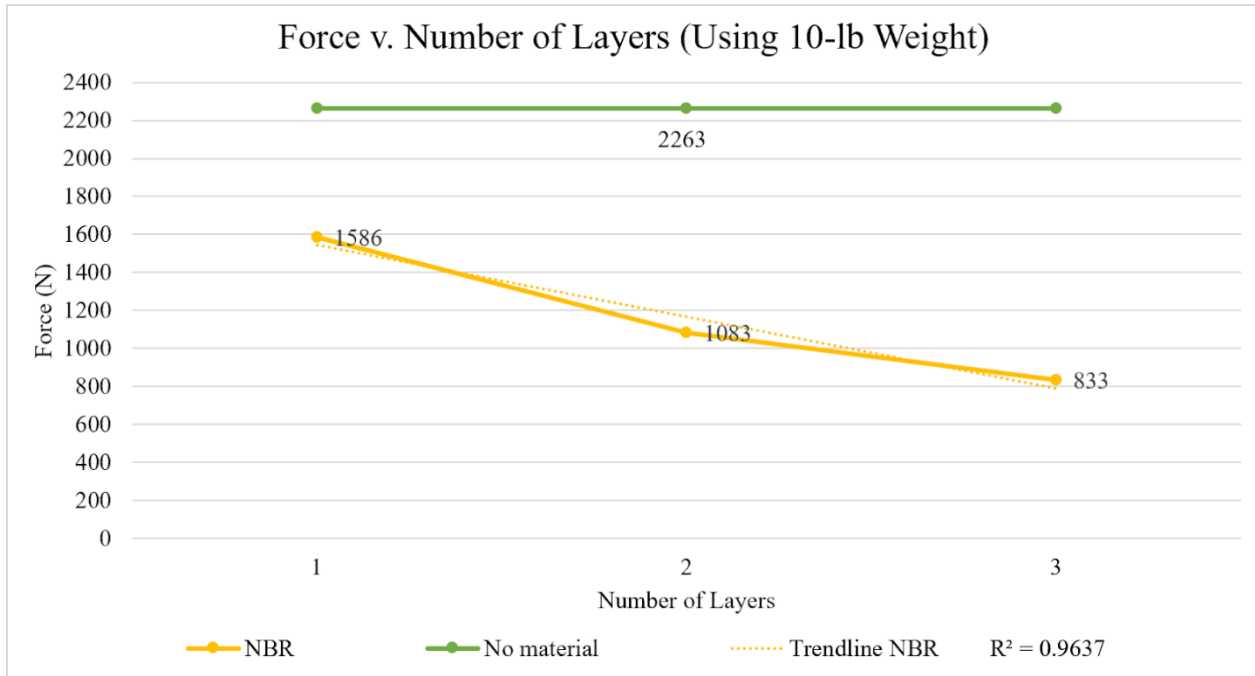


Figure 43. Measured vertical impact force values (N) from NBR and no material test conditions using a 10-lb weight

As seen in Figures 42 and 43, the green lines illustrate the constant impact force of the weights as they were dropped on the uncovered force plate. The orange lines each show a decreased slope as the impact force is reduced by the increasing number of NBR foam layers. Both trendlines for the NBR show a linear relationship as indicated by the R^2 values of 0.9697 and 0.9637 for the 5-lb and 10-lb weight, respectively.

6. Final Design and Validation

6.1 Final Design Architecture



Figure 44. Final design prototype

The shock absorbing brace, shown by Figure 44, that was built and tested for this project is composed of two cuffs: a thigh and a calf cuff. The cuffs are composed of aluminum 1100 and their inner diameters are covered in neoprene. The entirety of the cuffs are covered in a polyester spandex sleeve. The cuffs also have four slits, two on each side, through which one velcro strap can be attached. The velcro strap is attached to one side and it wraps around the front of the leg and goes through the slit on the opposite side of the cuff to secure the brace to the leg. The side of the velcro strap that touches the leg is also lined with a silicone non-slip band to prevent the cuff from sliding down the leg.

Stainless steel joints are attached to the backs of the cuffs. A glass-infused polycarbonate rod connects the thigh and the bottom cuffs and is attached to the cuffs by joints. The telescopic rod is composed of two pieces: a 0.3-inch diameter solid rod that fits into a hollow rod that has a 0.3-inch inner diameter and a 0.6-inch outer diameter. The solid rod is lined with two nitrile rubber disks that are two inches in diameter and are 1.18 in in thickness. The end of the hollow diameter rod contains a flat, 2-inch diameter end plate that compresses the nitrile rubber disks. A plastic stopper is also placed on the solid rod to ensure that the nitrile rubber disks compress uniformly. When worn, the brace is located at the back of the knee. When the knee is extended, the telescopic rods are also extended to their maximum length.

When the knee is flexed, the solid rod will be pushed inside the hollow rod, which will in turn compress the nitrile rubber disks.

6.2 Design Validation

6.2.1 Skin Electromyography Validation

Electromyography (EMG) is a type of test that measures response and electrical activity of a muscle. Specifically, EMG measures the nerve's stimulation in the muscle, and detects the muscle's action potentials during eccentric, concentric, or isometric muscle activation. The team performed EMG testing with surface electrodes on the skin to record muscle activity of the *vastus lateralis*, *vastus medialis*, and *rectus femoris*. These muscles were selected because they are integral muscles that contribute to the overall quadriceps' tendon force, the force (in addition to the patellar tendon force) that generates the patellofemoral joint resultant force. Moreover, this joint resultant force is dependent, biomechanically, upon the EMG activity of these muscles since generated muscle force can be linearly correlated to EMG muscle activation [72] [73]. The skin EMG tests were performed for the three above-mentioned muscles at four different activities: treadmill running (4 mph at no incline), forward lunging in place, squats, and stair climbing. Furthermore, EMG muscle activation during these activities was measured with and without the team's shock absorbing brace as well as with the gold standard, market equivalent DonJoy Reaction Web brace.

Fresh, disposable surface electrodes were placed on clean skin superficial to *vastus lateralis*, *vastus medialis*, and *rectus femoris*. The cleaning process involved wiping the area of application with a slightly abrasive alcohol wipe to remove any residual dirt, oil, or dead skin that would alter the connection between each electrode and skin, thus attenuating the EMG signals and contributing to potential signal noise. Once the electrode application sites were prepared, the positive and negative electrodes were placed on the skin superficial to the bellies of three muscles. This would attain the most representative signals of each of these muscles during testing and would help avoid measuring EMG activation of peripheral muscles within this anatomical region. Since bone does not generate EMG activity, the ground electrodes were attached to clean skin superficial to the lateral malleolus to serve as ground reference points for the positive and negative electrodes. The EMG data were collected using a Vernier EKG/EMG sensor with a LoggerPro data analysis software package. Wires from the Vernier EKG/EMG sensor were connected to the positive, negative, and ground electrode contact points using micro alligator clips. Within the LoggerPro data analysis program, EMG signals were measured using the sensor's maximum sampling rate of 200 samples/second, to achieve the highest signal accuracy, with a

test duration of 30 seconds. The acquired data from the LoggerPro software during testing were then exported to an Excel spreadsheet for future data and statistical analysis purposes.

Given the linear relationship between measured EMG activity and generated muscle force, the team was able to make initial conclusions relating EMG activity with muscle force for each of these muscles. Observing a change or no change in muscle activity, and thus muscle force, allowed the team to make assumptions about how changes in *vastus lateralis*, *vastus medialis*, and *rectus femoris* forces would affect the overall patellofemoral joint resultant force. Moreover, by comparing EMG muscle activity for each of the test cases (the team's shock absorbing brace versus no brace control and DonJoy Reaction Web brace), the team gained a clearer understanding of the advantages and limitations of our brace with respect to mitigating muscle force generation and the overall patellofemoral joint resultant force during various activities.

Due to the limitations of COVID-19, the team was only able to test the brace with healthy individuals. As expected in a healthy subject, we did not measure a significant change in EMG activity when comparing our brace versus the no brace control. Therefore, we compared our brace with the DonJoy Reaction Web brace and observed favorable results. Biomechanically, the patellofemoral joint resultant force is dependent on the *vastus lateralis*, *vastus medialis*, and *rectus femoris* activity since muscle force can be linearly correlated to muscle activity. From our skin EMG testing, we observed a favorable decrease in muscle activity, and thus decreased forces, for all three muscles in lunges, squats, and stair climbing activities for our final design brace prototype. These initial results were certainly promising in that muscle activity and force decrease in these three muscles were evident with our brace compared with the gold standard DonJoy brace, indicating that our brace reduced the overall patellofemoral joint resultant force. It is important to note that further testing (prevented due to COVID-19) with patients who have patellofemoral pain is needed in order to further validate that our brace was able to reduce the forces of these three muscles and, therefore, the overall patellofemoral joint resultant force.

6.2.2 Force Plate Validation

A force plate is a type of mechanical sensing equipment that utilizes one or more load cells to measure ground reaction forces of bodies that are placed upon it [74]. For the purpose of our project, the team used a force plate to determine the impact absorption ability of the nitrile rubber (NBR) foam. This testing was crucial for our final design validation since the purpose of the NBR foam was to help reduce the PF joint resultant force by absorbing the impact forces generated during active knee flexion. The impact force was measured for one, two, and three layers of NBR foam as well as with a no foam (control

case) placed on the force plate with 5-lb and 10-lb weights dropped from a consistent height of 12 inches.

The team used a single AMTI force plate and AMTI software package to perform the impact force testing and data analysis. To generate the impact force that the brace’s NBR foam would aim to absorb during knee flexion, the team performed separate tests using 5-lb and 10-lb barbell weight plates that were released onto the force plate from a height of 12 inches. First, a single layer (2 inches) of NBR foam was placed on the center of the force plate, the region which measures the most accurate ground reaction forces due to the positioning of the load cells within the device. A PVC pipe with a diameter similar to the diameter of the barbell plate’s hole was positioned through the center of the barbell plate to help properly track its freefall onto the force plate after release. This would promote the barbell plate to generate a uniformly distributed normal load on the NBR foam and/or force plate by landing at a near zero-degree angle, as opposed to landing at an angle which would generate an unevenly distributed force. This is important to replicate since the brace’s NBR foam would experience uniformly distributed normal loads during knee flexion. Prior to testing, the device was zeroed with one team member holding the PVC pipe on the center of the plate from the top and the weight held at the height of 12 inches. Once the force plate was zeroed, the team began to record data in the AMTI software and the weight was subsequently dropped. This process was repeated five times consecutively. After the weight was dropped for the fifth time in the trial, the data recording was stopped in the software. The measured data from the AMTI software during testing were then exported to an Excel spreadsheet for future data and statistical analysis purposes. The entire testing procedure outlined in this paragraph was completed for four NBR foam layer test cases (no layer control, one layer, two layers, three layers) for each barbell weight (5-lb or 10-lb).

This force plate testing results, evident in Table 9, provided the team with a clearer understanding of the NBR foam’s ability to dissipate impact forces of different magnitudes, since each activity (treadmill running, lunges, squats, stair climbing) generates different impact forces within the patellofemoral joint. Furthermore, after analyzing the acquired quantitative testing data, the team determined that two layers of NBR foam would be most suitable for our final brace design. Although three layers of NBR foam absorbs more impact force than two layers, knee range of motion would be limited with three layers compared with two layers of foam.

Table 9. Percent impact force reduced with increasing number of layers of NBR foam for the 5- and 10-lb weight tests

Number of Layers of NBR Shock Absorbing Foam	% Impact Force Reduced	
	5-lb Weight Test	10-lb Weight Test
1	8.3%	29.9%
2	31.2%	52.1%
3	43.4%	63.2%

Evident in our testing results above, incorporating two layers of NBR foam was appropriate for our final design because it was able to reduce impact force by more than 30% and 50% in the 5-lb and 10-lb weight impact tests, respectively. Additionally, using two layers of NBR foam does not inhibit normal knee flexion during treadmill running, lunges, squats, and stair climbing, based on subject feedback during these activities.

6.2.3 Statistical Analysis

Without further analysis of the data, it is difficult to determine if the differences observed in mean electrical activity between the three conditions (wearing the team’s brace, wearing the DonJoy Reaction Web Brace, and not wearing a brace) are statistically significant. As a result, the team conducted two-tailed t-tests assuming equal variances, with a confidence level of 95%, using the Data Analysis add-in in Microsoft Excel. The following hypotheses were also established:

- Null Hypothesis (H_0): Using the brace **does not** affect the average EMG signal of the *vastus lateralis/medialis* and *rectus femoris* muscles.
- Alternate Hypothesis (H_A): Using the brace **does** affect the average EMG signal of the *vastus lateralis/medialis* and *rectus femoris* muscles.

With these hypotheses, a p-value of less than 0.05 would reject the null hypothesis, therefore indicating the difference observed in mean electrical activity is significant. A p-value greater than or equal to 0.05 would indicate the alternate hypothesis is weak, and that the null hypothesis is not rejected.

Table 10 compares the mean EMG *rectus femoris* signals for the prototype brace and no brace conditions, and details the conclusions drawn from the p-value results of the two-tailed t-tests.

Table 10. Mean *rectus femoris* signal (Prototype Brace vs. No Brace)

Activity →	Squat	Lunges	Stairs	Treadmill
Prototype Brace (mean signal in mV)	0.0280	-	0.0210	0.6588
No Brace (mean signal in mV)	0.0279	-	0.0155	0.9103
p-value	0.9980	-	0.1533	0.1832
Conclusion	Fail to reject H_0 , no significant difference in signal observed.	-	Fail to reject H_0 , no significant difference in signal observed.	Fail to reject H_0 , no significant difference in signal observed.

The two-tailed t-tests ultimately concluded that there is no significant difference ($p > 0.05$) in *rectus femoris* activity while performing a squat, stair climb, or treadmill run with or without the prototype brace. *Rectus femoris* signal measurements were not obtained for lunges due to project limitations.

Table 11 compares the mean EMG *rectus femoris* signals for the prototype brace and Reaction Web Brace conditions, and details the conclusions drawn from the p-value results of the two-tailed t-tests.

Table 11. Mean *rectus femoris* signal (Prototype Brace vs. Reaction Web Brace)

Activity →	Squat	Lunges	Stairs	Treadmill
Prototype Brace (mean signal in mV)	0.0280	N/A	0.0210	0.6588
Reaction Web Brace (mean signal in mV)	0.0459	N/A	0.5073	0.8388
p-value	0.0004	N/A	3.3×10^{-5}	0.0810
Conclusion	Reject H_0 , significant decrease in signal observed compared to web brace.	N/A	Reject H_0 , significant decrease in signal observed compared to web brace.	Fail to reject H_0 , no significant difference in signal observed.

The two-tailed t-tests ultimately concluded there is a significant difference in *rectus femoris* activity observed between values obtained while wearing the prototype brace and the Reaction Web Brace when performing a squat and stair climb. In both activities, there was a significant ($p < 0.05$) decrease in signal observed while wearing the prototype brace in comparison to those obtained while wearing the Reaction Web Brace. The two-tailed t-test comparing *rectus femoris* signals during a treadmill run, however, concluded there was no significant difference ($p > 0.05$). *Rectus femoris* signal measurements were also not obtained for lunges due to project limitations.

Table 12 compares the mean EMG *vastus medialis* signals for the prototype brace and no brace conditions, and details the conclusions drawn from the p-value results of the two-tailed t-tests.

Table 12. Mean vastus medialis signal (Prototype Brace vs. No Brace)

Activity →	Squat	Lunges	Stairs	Treadmill
Prototype Brace (mean signal in mV)	0.0161	0.0260	0.0130	0.5988
No Brace (mean signal in mV)	0.0281	0.0468	0.0208	0.7465
p-value	0.0306	0.0071	0.0813	0.1346
Conclusion	Reject H_0 , significant increase in signal observed compared to no brace.	Reject H_0 , significant increase in signal observed compared to no brace.	Fail to reject H_0 , no significant difference in signal observed.	Fail to reject H_0 , no significant difference in signal observed.

The two-tailed t-tests ultimately concluded there is a significant difference ($p < 0.05$) in *vastus medialis* activity observed between values obtained while wearing the prototype brace and the Reaction Web Brace when performing a squat and lunge and no significant difference ($p > 0.05$) observed when performing a stair climb or treadmill run. There was a significant increase in vastus medialis signals while wearing the brace and performing a squat and lunge.

Table 13 compares the mean EMG *vastus medialis* signals for the prototype brace and Reaction Web Brace conditions, and details the conclusions drawn from the p-value results of the two-tailed t-tests.

Table 13. Mean vastus medialis signal (Prototype Brace vs. Reaction Web Brace)

Activity →	Squat	Lunges	Stairs	Treadmill
Prototype Brace (mean signal in mV)	0.0161	0.0260	0.0130	0.5988
Reaction Web Brace (mean signal in mV)	0.3219	0.7299	0.6357	0.8723
p-value	0.0015	2.2×10^{-5}	0.001	0.1060
Conclusion	Reject H_0 , significant decrease in signal observed compared to web brace.	Reject H_0 , significant decrease in signal observed compared to web brace.	Reject H_0 , significant decrease in signal observed compared to web brace.	Fail to reject H_0 , no significant difference in signal observed.

When comparing the prototype brace to the Reaction Web Brace, the two-tailed t-tests yielded p-values less than 0.05 for the squat, lunge, and stair activities, all indicating the decrease in *vastus medialis* signal when wearing the prototype brace in comparison to the web brace is significant. While performing a treadmill run, however, there was no significant difference in signal observed ($p > 0.05$).

Table 14 compares the mean EMG *vastus lateralis* signals for the prototype brace and no brace conditions, and details the conclusions drawn from the p-value results of the two-tailed t-tests.

Table 14. Mean *vastus lateralis* signal (Prototype Brace vs. No Brace)

Activity →	Squat	Lunges	Stairs	Treadmill
Prototype Brace (mean signal in mV)	0.0477	0.0526	0.0221	1.7291
No Brace (mean signal in mV)	0.0266	0.0493	0.0218	0.9319
p-value	0.1842	0.0042	0.9410	0.0350
Conclusion	Fail to reject H_0 , no significant difference in signal observed.	Reject H_0 , significant increase in signal observed compared to no brace.	Fail to reject H_0 , no significant difference in signal observed.	Reject H_0 , significant increase in signal observed compared to no brace.

The mean average *vastus lateralis* signals for the prototype brace and no brace conditions were found to be significantly different during the lunge and treadmill run activities ($p < 0.05$), with the prototype brace yielding higher EMG signals. During stair and squat activities, there was no significant difference in signal observed ($p > 0.05$).

Table 15 compares the mean EMG *vastus lateralis* signals for the prototype brace and no brace conditions, and details the conclusions drawn from the p-value results of the two-tailed t-tests.

Table 15. Mean *vastus lateralis* signal (Prototype Brace vs. Reaction Web Brace)

Activity →	Squat	Lunges	Stairs	Treadmill
Prototype Brace (mean signal in mV)	0.0477	0.0526	0.0221	1.7291
Reaction Web Brace (mean signal in mV)	0.2937	0.5885	0.4260	1.090

p-value	0.0022	0.0037	0.0002	0.0533
Conclusion	Reject H_0 , significant decrease in signal observed compared to web brace.	Reject H_0 , significant decrease in signal observed compared to web brace.	Reject H_0 , significant decrease in signal observed compared to web brace.	Fail to reject H_0 , no significant difference in signal observed.

In comparison to the Reaction Web Brace, the prototype brace yielded a significant decrease ($p < 0.05$) in *vastus lateralis* signals during the squat, lunge, and stair climbing activities; however, there was no significant difference ($p > 0.05$) observed during the treadmill run.

A statistical analysis was also conducted to verify the significance of the force plate data obtained. Similar to the skin EMG data, the team conducted two-tailed t-tests assuming equal variances, with a confidence level of 95%, using the Data Analysis add-in in Microsoft Excel. The following hypotheses were also established:

- Null Hypothesis (H_0): The addition of nitrile rubber foam **does not** affect the impact force recorded by the force plate.
- Alternate Hypothesis (H_A): The addition of nitrile rubber foam **does** affect the impact force recorded by the force plate.

With these hypotheses, a p-value of less than 0.05 would reject the null hypothesis, therefore indicating the difference observed in mean impact force values is significant. A p-value greater than or equal to 0.05 would indicate the alternate hypothesis is weak, and that the null hypothesis is not rejected.

Table 16 compares, in a two-tailed t-test, the mean impact forces recorded by the force plate when a 5-lb weight is dropped onto it without any shock absorbing material and with one, two, and three layers of the shock absorbing material, the nitrile rubber foam, and details the conclusions drawn by the resulting p-values.

Table 16. Mean impact force, 5-lb Drop Test

Number of layers of material →	1	2	3
Force (N)	950.1	712.6	586.5
Force, No Material (N)	1036.1	1036.1	1036.1
p-value	6.53×10^{-6}	1.16×10^{-10}	5.59×10^{-15}
Conclusion	Reject H_0 , significant decrease in impact forces compared to no material.	Reject H_0 , significant decrease in impact forces compared to no material.	Reject H_0 , significant decrease in impact forces compared to no material.

In comparison to the impact force recorded when there is no material on the force plate, each trial with differing amounts of material yielded significant decreases ($p < 0.05$) in impact forces.

Table 17 compares, in a two-tailed t-test, the mean impact forces recorded by the force plate when a 10-lb weight is dropped onto it without any shock absorbing material and with one, two, and three layers of the shock absorbing material, the nitrile rubber foam, and details the conclusions drawn by the resulting p-values.

Table 17. Mean impact force, 10-lb Drop Test

Number of layers of material →	1	2	3
Force (N)	1586.2	1083.0	833.3
Force, No Material (N)	2262.7	2262.7	2262.7
p-value	4.98×10^{-11}	1.12×10^{-17}	8.76×10^{-18}
Conclusion	Reject H_0 , significant decrease in impact forces compared to no material.	Reject H_0 , significant decrease in impact forces compared to no material.	Reject H_0 , significant decrease in impact forces compared to no material.

Similar to the 5-lb drop test, in comparison to the impact force recorded when there is no material on the force plate, each trial with differing amounts of material yielded significant ($p < 0.05$) decreases in impact forces.

6.3 Impacts of Final Design

6.3.1 Economics

The results of our project would not have an impact on the economy of everyday living. If the product were to become patented and sold on the market, its further development can produce jobs, which can positively impact economic status on an individual level. This aspect is further discussed in Section 6.3.3.

6.3.2 Environmental Impact

The shock-absorbing knee brace is composed of stainless steel, aluminum 1100, glass-infused polycarbonate and nitrile rubber foam. Stainless steel, aluminum 1100 and the glass-infused polycarbonate are all recyclable materials [75]. NBR is composed of acrylonitrile and butadiene. Some rubber manufacturing companies are beginning to use renewable raw materials to create butadiene, which can lessen the negative environmental impact. Rubber Recycling necessitates the use of toxic chemicals

and high temperatures, which is why it is not a popular method of disposing of rubber products. Nonetheless, rubber can be mechanically broken down and reused for another purpose or it can be burned and used for energy. Synthetic rubber, like NBR, also burns cleanly without releasing many toxic by-products. With time, technologies will also advance to find more environmentally friendly ways to dispose of synthetic rubbers like NBR [76].

6.3.3 Societal Impact

If our product were patented and started to be made by a company, its further development and manufacture could create potential jobs. The prototype of the current shock absorbing brace could also be further designed and improved by other engineers. Additionally, if the manufacturing process of the brace were to become automated, individuals would need to be hired to create the machines that build the brace. Once those are up and running, they would still need constant surveillance to ensure that they run smoothly, which can open up additional job roles. Given the extent to which the current prototype is developed, if this project were to be manufactured and placed on the market, a variety of individuals would need to be employed to make it possible.

6.3.4 Political Ramifications

Our product would not have any effect on the culture of other countries.

6.3.5 Ethical Concerns

Our product was designed with the goal of reducing the compressive force on the patellofemoral joint, which has the potential to alleviate patellofemoral pain and prevent the early development of osteoarthritis. Wearing the brace can enable individuals to return to an active lifestyle that they may have to compromise due to their PF pain. Likewise, the shock absorbing brace can allow wearers to continue their physical activity even as they age, which they may not have been able to do without it. The product itself does not raise ethical concerns. If testing of the current or future product iterations were done on patients with patellofemoral pain, the test subjects would be provided with a full disclosure of the tests they would participate in and what any potential risks are. Additionally, the test subjects would be selected on a volunteer basis, which would ensure that any product testing is done ethically.

6.3.6 Health and Safety Issues

The shock absorbing brace is intended to alleviate patellofemoral pain. By using the brace during physical activity, individuals should feel their patellofemoral joint supported and experience a reduction

in the compressive force on the joint. This can allow wearers to increase the amount of physical activity they can do without experiencing pain, which will have an overall positive effect on their lifestyle. In addition to increasing activity, the brace can help prevent further patellofemoral complications, such as osteoarthritis since the shock absorbing mechanism helps reduce the friction between the femur and patella.

6.3.7 Manufacturability

The telescopic rod of the shock absorber brace was manufactured using a CNC lathe while the metal cuffs were cut using a CNC mill. The joints were attached to the cuffs and the telescopic rod using screws. The outer shape of the NBR foam was cut using a circular stamp cutting device and a mechanic drill was used to cut the hole in the middle of the foam disks. The neoprene was attached to the inside of the cuffs using hot glue. The cuff coverings were made with polyester spandex and hot glue, but ideally, they would have been sewn together. The non-slip material was also hot-glued to the back of the velcro buckles, which were manually attached to the cuffs. Given the simplicity of the device development, its manufacturability on a larger scale is possible. A similar prototype could be easily made with the equipment available at WPI. If the product were to become patented and reproduced on a much larger scale, an automated process could be developed to help manufacture the braces faster and more efficiently.

6.3.8 Sustainability

Our product would not have an influence on the environment in regards to renewable energy.

7. Discussion

7.1. Project Limitations

7.1.1 Human Subject Limitations

The team was subject to several limitations in the testing process. Test subjects for this project were limited to female members of the project team, none of which have diagnosed PFPS. Ideal test subjects would have included patients of varying heights, ages, and genders who experience patellofemoral pain; however, this would have required a professional diagnosis or voluntary disclosure of patellofemoral pain and subsequent anonymization of test subject identities and results. Furthermore, testing of this nature would have required IRB (Institutional Review Board) approval, which was not feasible in the scope of this project. Without testing subjects with diagnosed PFPS, the data collected may not reflect the most accurate results for EMG signal testing. Since the testing occurred on healthy individuals, muscle activation for the tested muscles (*vastus lateralis*, *vastus medialis*, and *rectus femoris*) may differ drastically enough to skew data. The only way to prove or disprove this would be to expand the testing to PFPS demographics with the proper approval.

For more accurate test results, the team considered the use of intramuscular EMG electrodes; however, due to the invasive nature of this test and the need for a trained medical professional, the team opted to pursue the less invasive, skin EMG route. The team also researched ways to accurately measure the force between the patella and trochlear groove, but similarly to the use of intramuscular EMG electrodes, such testing would likely be invasive and cause discomfort to the test subject.

7.1.2 Assumptions

Throughout the validation testing of the shock absorbing brace, the team assumed that the exercises performed during EMG testing were universal. This assumption indicates that the exercises done, such as running, stair climbing, squatting, and lunging were done the same way that they would be done by any other individual. Additionally, during the EMG testing, it was assumed that the exercises were performed the same each time: both between test subjects and within the same repetition of exercises performed by the same subject.

8. Conclusion and Recommendations

8.1 Future Work

Due to the repercussions of COVID-19 on the WPI community, the team was limited in their data collection. While preliminary testing was conducted and analyzed, various tests needed to be clarified and redone in order to further validate the project. Also, while the design of the shock-absorbing knee brace met the project objectives, there are other improvements that could be made to further develop the design. The following are areas of future work that the team recommends:

- **Human Subject Testing:** As stated in section 7.1.1, the pool of test subjects for this project were limited due to a variety of criteria. Three healthy females were used to collect the preliminary data captured in this report, but ideally the pool of subjects should be expanded to include subjects with PFPS in order to yield more solid results. Additionally, there should be variability in age, gender, and activity level for further tests.
- **Design Validation:** In order to clarify and support the hypotheses laid out in this report, design validation testing should be performed. The use of cadaveric specimens is recommended in order to gain a more in-depth anatomical picture of the brace's effects on the patellofemoral joint. Also, invasive testing techniques such as intramuscular EMGs should be utilized. As stated in section 7.1.1, invasive techniques can give a more accurate result than skin EMGs. Finally, durability testing should be performed on the brace. These tests would include various cyclic loading test procedures that would validate the lifespan of the brace.
- **Improved Design and Adjustability:** The design of the brace can be manipulated to be better suited for manufacturability, as well as adjustable fits for different sized athletes. The components of the brace (thigh and calf cuffs, telescopic rod, NBR foam) can be given different dimensions.

8.2 Conclusions

Through the course of the project, the team developed a shock-absorbing brace to unload the compressive forces on the patellofemoral joint due to physical activity. The device designed showed promising results compared to the gold standard market equivalent, the DonJoy Reaction Web Brace; according to the EMG data collected, the team's product decreased muscle activity for the *vastus medialis*, *vastus lateralis* and *rectus femoris* while performing lunges, squats and stair climbing. Results comparing the team's brace to wearing no brace did not display significant results due during the testing cycle conducted; while wearing the team's brace, there was either no change in the activity of these

muscles or an increase in muscle activity. However, due to an inability to perform further testing on more subjects as a result of COVID-19, future testing will be needed.

References

- [1] G. Waryasz and A. Y. Mcdermott, "Patellofemoral pain syndrome (PFPS): a systematic review of anatomy and potential risk factors," *Dynamic Medicine*, vol. 7, no. 1, 2008.
- [2] W.-C. S and A. G., United States Bone and Joint Initiative: The Burden of Musculoskeletal Diseases in the United States (BMUS)., 2014.
- [3] F. Halabchi, R. Mazaheri and T. Seif-Barghi, "Patellofemoral Pain Syndrome and Modifiable Intrinsic Risk Factors; How to Assess and Address?," *Asian Journal of Sports Medicine*, vol. 4, no. 2, 2013.
- [4] F. Halabchi, M. Abolhasani, M. Mirshahi and Z. Alizadeh, "Patellofemoral pain in athletes: clinical perspectives," *Open Access Journal of Sports Medicine*, vol. 8, pp. 189-203, 2017.
- [5] K. DeHaven and D. Lintner, "Athletic injuries: comparison by age, sport, and gender," *Am J Sports Medicine*, vol. 14, no. 3, pp. 218-224, 1986.
- [6] A. Amoako and G. Pujalte, "Osteoarthritis in Young, Active, and Athletic Individuals," *Clinical Medicine Insights: Arthritis and Musculoskeletal Disorders*, vol. 7, p. 27–32, 2014.
- [7] M. J. Thomas, L. Wood, J. Selfe and G. Peat, "Anterior knee pain in younger adults as a precursor to subsequent patellofemoral osteoarthritis: a systematic review," *BMC Musculoskeletal Disorders*, vol. 11, no. 1, 2010.
- [8] E. Losina *et. al*, "Lifetime Medical Costs of Knee Osteoarthritis Management in the United States: Impact of Extending Indications for Total Knee Arthroplasty," *Arthritis Care Res (Hoboken)*, vol. 67, pp. 203-215, 2015.
- [9] E. N. Marieb, K. Hoehn and M. Hutchinson, Human anatomy & physiology, 9th edition, Harlow, Essex: Pearson, 2014.
- [10] P. F. Harris, C. Ranson and A. Robertson, Anatomy for problem solving in sports medicine: the knee, Keswick, Cumbria: M & K Update Ltd, 2014.
- [11] J. Loudon, "BIOMECHANICS AND PATHOMECHANICS OF THE PATELLOFEMORAL JOINT," *Int J Sports Phys Ther.*, vol. 11, no. 6, p. 820–830, 2016.
- [12] R. A. Pedowitz, J. J. O'Connor and W. H. Akeson, Knee Injuries: Ligament and Cartilage Structure, Function, Injury, and Repair, Philadelphia: Wolters Kluwer, 2015.
- [13] J. Abulhasan and M. Grey, "Anatomy and Physiology of Knee Stability," *Journal of Functional Morphology and Kinesiology*, vol. 2, no. 4, p. 34, 2017.
- [14] M. F. Reinking, "CURRENT CONCEPTS IN THE TREATMENT OF PATELLAR TENDINOPATHY," *International journal of sports physical therapy* , vol. 11, no. 6, pp. 854-866, 2016.

- [15] A. Fox *et al.*, "The Basic Science of Articular Cartilage: Structure, Composition, and Function," *Sports Health: A Multidisciplinary Approach*, vol. 1, no. 6, p. 461–468, 2009.
- [16] P. Chatra, "Bursae around the Knee Joints," *Indian Journal of Radiology and Imaging*, vol. 22, no. 1, p. 27, 2012.
- [17] J. Kiel and K. Kaiser, Patellofemoral Arthritis, StatPearl, 2019.
- [18] S. F. Habusta and E. E. Griffin, Chondromalacia Patella, Treasure Island, FL: StatPearls Publishing, 2019.
- [19] E. Bass, "Tendinopathy: Why the Difference Between Tendinitis and Tendinosis Matters," *The International Journal of Therapeutic Massage & Bodywork*, vol. 5, pp. 14-17, 2012.
- [20] D. P. Johnson, C. J. Wakeley and I. Watt, "Magnetic Resonance Imaging Of Patellar Tendonitis," *The Journal of Bone and Joint Surgery*, vol. 78, no. 3, pp. 452-457, 1995.
- [21] I. J. Tiemessen, P. P. F. Kuijer, C. T. Hulshof and M. H. Frings-Dresen, "Risk factors for developing jumpers knee in sport and occupation: a review," *BMC Research Notes*, vol. 2, no. 1, p. 127, 2009.
- [22] M. Blazina, R. Kerlan, F. Jobe, V. Carter and G. Carlson, "Jumper's knee," *Orthop Clin North Am*, no. 4, pp. 665-678, 1973.
- [23] D. Hunter, Y. Zhang and J. Niu *et. al.*, "Patella malalignment, pain and patellofemoral progression: the Health ABC Study," *Osteoarthritis Cartilage*, vol. 15, no. 10, pp. 1120-1127, 2007.
- [24] G. Gasparini, F. Familiari and F. Ranuccio, " Patellar malalignment treatment in total knee arthroplasty," *Joints*, vol. 1, no. 1, pp. 10-17, 2013.
- [25] M. Saper and D. Shneider, "Diagnosis and treatment of lateral patellar compression syndrome," *Arthrosc Tech*, vol. 3, no. 5, pp. 633-638, 2014.
- [26] H. Singh, M. Mckay, J. Baldwin, L. Nicholson, C. Chan, J. Burns and C. E. Hiller, "Beighton scores and cut-offs across the lifespan: cross-sectional study of an Australian population," *Rheumatology*, vol. 57, no. 11, pp. 1857-1864, 2017.
- [27] H. Saremi, A. Yavarikia and N. Jafari, "Generalized Ligamentous Laxity: An Important Predisposing Factor for Shoulder Injuries in Athletes," *Iranian Red Crescent Medical Journal*, vol. 18, no. 6, 2016.
- [28] K. J. Murray, "Hypermobility disorders in children and adolescents," *Best Practice & Research Clinical Rheumatology*, vol. 20, no. 2, pp. 329-351, 2016.
- [29] V. Pacey, L. Tofts, R. D. Adams, C. F. Munns and L. L. Nicholson, "Exercise in children with joint hypermobility syndrome and knee pain: a randomised controlled trial comparing exercise into hypermobile versus neutral knee extension," *Pediatric Rheumatology*, vol. 11, no. 1, 2013.

- [30] "Tru-Pull Advanced System Brace," DJO Global, 2019. [Online]. Available: <https://www.djoglobal.com/products/donjoy/tru-pull-advanced-system>.
- [31] "Reaction Web Knee Brace," 2019. [Online]. Available: <http://www.djoglobal.com/products/donjoy/reaction-web-knee-brace>.
- [32] "Form Fit Knee Hinged Lateral J Brace," 2019. [Online]. Available: <https://www.ossur.com/en-us/bracing-and-supports/knee/formfit-hinged-knees>.
- [33] "FX Patella Stabilizer Brace," 2019. [Online]. Available: <https://www.ossur.com/en-us/bracing-and-supports/knee/fx-stabilizer>.
- [34] "FreeRunner Knee Brace," 2019. [Online]. Available: <https://www.breg.com/products/knee-bracing/patellofemoral/freerunner-knee-brace/>.
- [35] Breg, "Tendon Compression Strap," Breg, [Online]. Available: <https://www.breg.com/products/knee-bracing/patellofemoral/tendon-compression-strap/>.
- [36] M. Walden, "Patellofemoral Pain Taping," Sports Injury Clinic, 29 June 2019. [Online]. Available: <https://www.sportsinjuryclinic.net/sport-injuries/knee-pain/anterior-knee-pain/patella-taping>.
- [37] Royal Australian College of General Practitioners, "Taping for Knee Osteoarthritis," RACGP, The Royal Australian College of General Practitioners, [Online]. Available: <https://www.racgp.org.au/afp/2013/october/taping-for-knee-osteoarthritis>.
- [38] K. Crossley, K. Bennell, S. Cowan and S. Green, "Analysis of outcome measures for persons with patellofemoral pain: which are reliable and valid?," *Archives of Physical Medicine and Rehabilitation*, vol. 85, no. 5, pp. 815-822, 2004.
- [39] M. McCarthy and S. Strickland, "Patellofemoral Pain: an Update on Diagnostic and Treatment Options," *Current Reviews in Musculoskeletal Medicine*, vol. 6, no. 2, pp. 188-194, 2013.
- [40] S. Ramamoorthy and J. Cidlowski, "Corticosteroids - Mechanisms of Action in Health and Disease," *Rheumatic Disease Clinics of North America*, vol. 42, no. 2, 2018.
- [41] P. Wehling, "Effectiveness of Intra-Articular Therapies in Osteoarthritis: a Literature Review," *Therapeutic Advances in Musculoskeletal Disease*, vol. 9, no. 8, pp. 183-196, 2017.
- [42] "US20170105865A1 - Customizable knee brace intended for patients with osteoarthritis," Google Patents, [Online]. Available: <https://patents.google.com/patent/US20170105865?q=web+knee+brace>.
- [43] B. Livolsi and E. Zirpolo-Kisco, "Patella strap and method of alleviating anterior knee pain". United States of America Patent US20060069337A1, 23 09 2005.
- [44] G. W. Johnson Jr., "Knee brace having adjustable inflatable U-shaped air cell". United States of America Patent US4872448A, 19 05 1987.

- [45] S. Singer and J. Fried, "Orthopaedic brace with an inflatable air bag". United States of America Patent US5558627A, 06 12 1993.
- [46] D. Dennis, "Range of motion after total knee arthroplasty: The effect of implant design and weight-bearing conditions," *The Journal of Arthroplasty*, vol. 13, no. 7, pp. 748-752, 1998.
- [47] T. Flynn and R. Soutas-Little, "Patellofemoral Joint Compressive Forces in Forward and Backward Running," *Journal of Orthopaedic and Sports Physical Therapy*, vol. 21, no. 5, pp. 277-282, 1995.
- [48] J. Roland, "How Much Does the Average Man Weigh," Healthline, 8 March 2019. [Online]. Available: <https://www.healthline.com/health/mens-health/average-weight-for-men>.
- [49] J. Karp, "Distance Running: How Many Miles Should You Run?," Active.com, 9 January 2013. [Online]. Available: <https://www.active.com/running/articles/distance-running-how-many-miles-should-you-run?page=2>.
- [50] W. Bumgardner, "How Many Steps Are There in a Mile?," Verywell Fit, 4 August 2019. [Online]. Available: <https://www.verywellfit.com/how-many-walking-steps-are-in-a-mile-3435916>.
- [51] "When Can You Replace a Knee Brace?," Össur Americas, [Online]. Available: <https://www.ossur.com/resources/ossur-r-r/when-can-you-replace-a-knee-brace>.
- [52] Standard Test Method for Performing Behind-the-Knee (BTK) Test for Evaluating Skin Irritation Response to Products and Materials That Come Into Repeated or Extended Contact with Skin, ASTM F2808, 2017.
- [53] Standard Guide for Accelerated Corrosion Testing for Mechanical Fasteners, ASTM F2832, 2016.
- [54] Standard Terminology Relating to Methods of Mechanical Testing, ASTM E6, 2015.
- [55] Standard Test Methods for Tension Testing of Metallic Materials, ASTM E8/E8M, 2016.
- [56] Standard Test Method for Air Permeability of Textile Fabrics, ASTM D737, 2018.
- [57] Limb Orthoses, 21 CFR 890.3475 US Food and Drug Administration, 2018.
- [58] Daily activity assistive device, 21 CFR 890.5050, US Food and Drug Administration, 2018.
- [59] External limb prostheses and external orthoses, ISO 21063, International Organization for Standardization, 2006.
- [60] Prosthetics and orthotics, ISO 21063, International Organization for Standardization, 2017.
- [61] Prosthetics and orthotics, ISO 13404, International Organization for Standardization, 2007.
- [62] Prosthetics and orthotics - Vocabulary - Part 1, ISO 854901, International Organization for Standardization, 1989.
- [63] Prosthetics and orthotics - Functional deficiencies, ISO 8551, International Organization for Standardization, 2003.

- [64] "Waterproof Ratings & Breathability Guide," Evo, [Online]. Available: <https://www.evo.com/guides/outerwear-waterproof-ratings-and-breathability#how-breathability-ratings-are-determined>.
- [65] "Aluminum," McMaster-Carr, [Online]. Available: <https://www.mcmaster.com/aluminum-sheets/corrosion-resistant-aluminum/easy-to-form-pure-1100-aluminum-sheets-and-bars-7/>.
- [66] "Neoprene Explained," Monmouth Rubber & Plastics, [Online]. Available: <https://monmouthrubber.com/neoprene-explained/>.
- [67] "Polycarbonate," McMaster-Carr, [Online]. Available: <https://www.mcmaster.com/polycarbonate/impact-resistant-polycarbonate/>.
- [68] "Dowel-Pins," McMaster-Carr, [Online]. Available: <https://www.mcmaster.com/dowel-pins/pins/dowel-pins-7/>.
- [69] D. Winter, *Biomechanics and Motor Control of Human Movement*, Hoboken, NJ: John Wiley, 2009.
- [70] A. Rambely, "Muscle Activity During Gait On a Treadmill," *International Conference on Biomechanics in Sports*, 2016.
- [71] L. Slater and J. Hart, "Muscle Activation Patterns During Different Squat Techniques," *Journal of Strength and Conditioning Research*, vol. 31, no. 3, pp. 667-676, 2017.
- [72] B. Alkner, P. Tesch and H. Berg, "Quadriceps EMG/force relationship in knee extension and leg press," *Medicine & Science in Sports & Exercise*, vol. 32, no. 2, p. 459, 2000.
- [73] T. Roberts and A. Gabaldon, "Interpreting muscle function from EMG: lessons learned from direct measurements of muscle force," *Integrative and Comparative Biology*, vol. 48, no. 2, pp. 312-320, 2008.
- [74] K. Lamkin-Kennard and M. Popovic, "Sensors: Natural and Synthetic Sensors," *Biomechatronics*, pp. 81-107, 2019.
- [75] "Polycarbonate Recycling - How is polycarbonate recycled?," Plastic Expert, [Online]. Available: <https://www.plasticexpert.co.uk/plastic-recycling/polycarbonate-recycling/>.
- [76] "Is Nitrile Butadiene Rubber a Sustainable Product?," Monmouth Rubber & Plastics, [Online]. Available: <https://monmouthrubber.com/is-nitrile-butadiene-rubber-a-sustainable-product/>.

Appendices

Appendix A: Equations and Calculations

1. Forces on the thigh without the brace

Calculations of thigh weight and center of mass from anthropometric data

$$\text{Weight of thigh} = W_{TH} = 0.1 (\text{body weight}) = 0.1 (64 \text{ kg}) = 6.4 \text{ kg} = 62.76 \text{ N}$$

$$\text{Center of mass of thigh} = r_{COMth} = 0.567 (\text{segment length}) = 0.567 (0.422 \text{ m}) = 0.239 \text{ m}$$

$$\text{Weight of upper body} = W_{UB} = 0.678 (\text{body weight}) = 0.678 (64 \text{ kg}) = 43.392 \text{ kg} = 425.55 \text{ N}$$

Solving for the force of the knee

$$\sum F_y = -F_{WUB} - F_{WT} + F_{Patella}(\sin 30^\circ) = 0 \quad (1)$$

$$0 = -425.55 \text{ N} - 62.76 \text{ N} + F_{Patella}(\sin 30^\circ)$$

$$F_{Patella} = (488.31 \text{ N}) \div (\sin 30^\circ)$$

$$F_{Patella} = 977 \text{ N}$$

2. Forces on the thigh with the brace

Solving for the force of the knee

$$\sum F_y = -F_{WUB} - F_{WT} + F_{BR}(\sin 45^\circ) + F_{Patella}(\sin 30^\circ) = 0 \quad (2)$$

$$F_{BR} = [(F_{WUB} + F_{WT} - F_{Patella}(\sin 30^\circ))] \div (\sin 45^\circ)$$

$$F_{BR} = (488.31 \text{ N} - F_{Patella}(\sin 30^\circ)) \div (\sin 45^\circ) \quad (3)$$

$$\sum M_A = M_{WUB} + M_{WT} - M_{Bry} = 0 \quad (4)$$

$$0 = (r_{TH} \times F_{WUB}) + (r_{COM(thigh)} \times F_{WT}) - (r_{BR} \times F_{BR} (\sin 45^\circ))$$

$$0 = (0.422 \text{ m})(425.55 \text{ N}) + (0.24 \text{ m})(62.76 \text{ N}) - r_{BR}(488.31 \text{ N} - F_{Patella}(\sin 30^\circ))$$

$$0 = 194.58 \text{ N}\cdot\text{m} - 0.225 \text{ m}(488.31 - F_{Patella}(\sin 30^\circ))$$

$$0 = 194.58 \text{ N}\cdot\text{m} - 109.87 \text{ N}\cdot\text{m} + 0.225(F_{Patella}(\sin 30^\circ))$$

$$0 = 84.71 \text{ N}\cdot\text{m} + 0.11(F_{Patella})$$

$$F_{Patella} = -753 \text{ N}$$

3. Design Optimization

Solving for the force supported by the brace at varied distances

$$\sum F_y = -F_{WUB} - F_{WT} + F_{BR}(\sin 45^\circ) + F_{Patella}(\sin 30^\circ) = 0 \quad (2)$$

$$F_{BR} = [(F_{WUB} + F_{WT} - F_{Patella}(\sin 30^\circ))] \div (\sin 45^\circ)$$

$$F_{BR} = (488.31 \text{ N} - F_{Patella}(\sin 30^\circ)) \div (\sin 45^\circ) \quad (3)$$

$$\sum M_A = M_{WUB} + M_{WT} - M_{Bry} = 0 \quad (4)$$

$$0 = (r_{TH} \times F_{WUB}) + (r_{COM(thigh)} \times F_{WT}) - (r_{BR} \times F_{BR}(\sin 45^\circ))$$

$$0 = (0.422 \text{ m})(425.55 \text{ N}) + (0.24 \text{ m})(62.76 \text{ N}) - r_{BR}(488.31 \text{ N} - F_{Patella}(\sin 30^\circ))$$

$$194.58 \text{ N}\cdot\text{m} = r_{BR}(488.31 - F_{Patella}(\sin 30^\circ))$$

$$F_{Patella} = -[(194.58 \div r_{BR}) - 488.31] \div (\sin 30^\circ)$$

Appendix B: Skin Electromyography Protocol

1. Prepare the skin for application of electrodes by wiping clean the surface and let dry.
2. The electrodes must be placed parallel to the muscle fibers below the skin. Place the electrodes on the vastus medialis, vastus lateralis, and rectus femoris with the correct orientation. The electrodes should have appropriate adhesive, but if more adhesion is needed, they may be secured with athletic tape.
3. A reference electrode must be secured to the body. This electrode should be placed over a bony landmark, in this case use the patella. The electric activity at this site will be filtered out as no muscle detection will occur.
4. Once electrodes are attached successfully, check that they are working properly when hooked up to the software. Move the leg slightly to see if readings are coming up on the monitor. If so, proceed with the testing.
5. Perform activities with and without the brace while connected to EMG.
6. Compare voltage output for tests done with and without the brace to see if brace has less activation of muscle. This will show if there is a reduction of force on the knee.

Appendix C: Nitrile Rubber Force Reduction – Force Plate Protocol

1. Turn on force plate and open AMTI software
2. Take a PVC pipe that has a 1-inch diameter
3. Place the 5-lb weight through the middle of the PVC pipe
4. Place the pipe at the origin on the force plate
5. Have an individual is holding the PVC pipe from the top
6. Zero the force plate
7. Begin recording date
8. Have another individual drop the weight from a height of 12 inches
9. Repeat Step 8 five times
10. Stop recording
11. Repeat Steps 7-10 three times
12. Download the data gathered from the AMTI software
13. Place one layer of nitrile rubber foam at the origin of the force plate
14. Repeat Steps 2-12 using one layer of nitrile rubber
15. Repeat Steps 2-12 using two layers of nitrile rubber
16. Repeat Steps 2-12 using three layers of nitrile rubber

Appendix D: Skin EMG Data

1. Rectus Femoris – Treadmill Testing (Average Maximum Peaks)

Subject #	Muscle		Leg With Brace	Average	Standard Dev	Leg Without Brace	Average	Standard Dev
1	RF	Brace	0.589423717			0.458248204		
1	RF	Brace	0.588764202			0.404258609		
1	RF	Brace	0.799938136			0.508668948		
2	RF	Brace	0.753233527			0.772302691		
2	RF	Brace	0.887449519			0.742667999		
2	RF	Brace	0.874943916			0.622740256		
3	RF	Brace	0.572992122			0.426857861		
3	RF	Brace	0.434522718			0.549278839		
3	RF	Brace	0.427813735	0.66	0.18	0.44576871	0.55	0.14
1	RF	No Brace	0.787607644			1.69505913		
1	RF	No Brace	0.807974213			1.528300644		
1	RF	No Brace	0.858417491			2.020033644		
2	RF	No Brace	1.52543312			0.732013126		
2	RF	No Brace	1.893413268			0.671913202		
2	RF	No Brace	1.36939137			0.571281746		
3	RF	No Brace	0.440895285			0.382237384		
3	RF	No Brace	0.363318218			0.372335614		
3	RF	No Brace	0.506696752			0.364371723		
1	RF	No Brace	0.549481316	0.91	0.52	0.463989929	0.88	0.62
1	RF	Web	0.919602189			1.171884387		
1	RF	Web	1.080050523			1.366400212		
1	RF	Web	1.124890828			1.129166842		
2	RF	Web	0.760907472			0.423601523		
2	RF	Web	0.89379528			0.557068226		
2	RF	Web	1.059046836			0.510775785		
3	RF	Web	0.600945887			0.417598367		
3	RF	Web	0.51795404			0.474732813		
3	RF	Web	0.592306281	0.84	0.23	0.41800275	0.72	0.39

2. Vastus Lateralis/Medialis – Treadmill Testing (Average Maximum Peaks)

Subject #	Muscle	Vastus Lateralis	Average	Standard Dev	Vastus Medialis	Average	Standard Dev
1	VLVM Brace	1.118659202			0.63532708		
1	VLVM Brace	1.328460187			0.768217414		
1	VLVM Brace	1.099341114			0.898496518		
2	VLVM Brace	2.350610261			0.55615134		
2	VLVM Brace	2.856587313			0.48996229		
2	VLVM Brace	2.937350305			0.717262397		
3	VLVM Brace	1.444416125			0.51612354		
3	VLVM Brace	1.359309917			0.421923512		
3	VLVM Brace	1.066962694	1.73	0.77	0.385497898	0.60	0.17
1	VLVM No Brace	2.037466202			1.037317732		
1	VLVM No Brace	0.837600979			0.912206139		
1	VLVM No Brace	0.820717393			1.068811404		
2	VLVM No Brace	0.612007013			0.785459501		
2	VLVM No Brace	0.995632448			0.637708206		
2	VLVM No Brace	2.131059825			0.746583064		
3	VLVM No Brace	0.349228131			0.549390649		
3	VLVM No Brace	0.314282853			0.458761574		
3	VLVM No Brace	0.288657721	0.93	0.70	0.522167413	0.75	0.22
1	VLVM Web	0.630328841			0.962765372		
1	VLVM Web	0.770326316			1.008387807		
1	VLVM Web	0.78099864			1.016024791		
2	VLVM Web	1.823607675			1.098993088		
2	VLVM Web	1.454387394			1.476868397		
2	VLVM Web	1.929214779			1.335913066		
3	VLVM Web	0.695648936			0.29480859		
3	VLVM Web	0.917936072			0.317359768		
3	VLVM Web	0.809883886	1.09	0.51	0.3397947	0.87	0.45

3. Rectus Femoris – Activity Testing (Average Maximum Peaks)

Muscle		Activity	Vastus Lateralis	Average	Standard Deviation	Vastus Medialis	Average	Standard Deviation
RF	Brace	Squat	0.024138152			0.025609377		
RF	Brace	Squat	0.030306685			0.028432915		
RF	Brace	Squat	0.029478353	0.03	0.003348001	0.0285291	0.03	0.001658634
RF	No Brace	Squat	0.022571404			0.024764924		
RF	No Brace	Squat	0.02662198			0.027042897		
RF	No Brace	Squat	0.034697225	0.03	0.006173226	0.025444572	0.03	0.001169453
RF	Web	Squat	0.41280953			0.253350246		
RF	Web	Squat	0.426717812			0.244318228		
RF	Web	Squat	0.538704146	0.46	0.069021535	0.702235501	0.40	0.261810293
RF	Brace	Stairs	0.016973673			0.011085713		
RF	Brace	Stairs	0.022409183			0.010605322		
RF	Brace	Stairs	0.023479206	0.02	0.003488354	0.00941745	0.01	0.00085877
RF	No Brace	Stairs	0.020197082			0.010267534		
RF	No Brace	Stairs	0.012954335			0.007074356		
RF	No Brace	Stairs	0.013404361	0.02	0.004057934	0.007136133	0.01	0.00182601
RF	Web	Stairs	0.48107505			0.314955861		
RF	Web	Stairs	0.486630736			0.423488186		
RF	Web	Stairs	0.554322438	0.51	0.04078033	0.745586529	0.49	0.223967773

4. Vastus Lateralis/Medialis – Activity Testing (Average Maximum Peaks)

Muscle	Activity	Vastus Lateralis	Average	Standard Deviation	Vastus Medialis	Average	Standard Deviation
VLVM	Brace Lunge	0.061089569			0.024095901		
VLVM	Brace Lunge	0.046587937			0.025648538		
VLVM	Brace Lunge	0.050126071	0.05	0.007561019	0.028225091	0.03	0.002085646
VLVM	No Brace Lunge	0.062701938			0.05208059		
VLVM	No Brace Lunge	0.038490064			0.039138697		
VLVM	No Brace Lunge	0.046638468	0.05	0.012319676	0.049217715	0.05	0.006797981
VLVM	Web Lunge	0.474994092			0.702310706		
VLVM	Web Lunge	0.528524682			0.695567821		
VLVM	Web Lunge	0.761850546	0.59	0.152530384	0.791866776	0.73	0.05375755
VLVM	Brace Squat	0.052151043			0.018850059		
VLVM	Brace Squat	0.043164844	0.05	0.006354202	0.013433372	0.02	0.003830176
VLVM	No Brace Squat	0.017713558			0.026423666		
VLVM	No Brace Squat	0.017171767			0.026134234		
VLVM	No Brace Squat	0.04485553	0.03	0.015829145	0.031714018	0.03	0.003141273
VLVM	Web Squat	0.264395955			0.302848597		
VLVM	Web Squat	0.287264365			0.36404531		
VLVM	Web Squat	0.32943092	0.29	0.032991234	0.29876483	0.32	0.036567872
VLVM	Brace Stairs	0.027462649			0.016047003		
VLVM	Brace Stairs	0.021294248			0.010588356		
VLVM	Brace Stairs	0.017430563	0.02	0.005059973	0.012234117	0.01	0.002800103
VLVM	No Brace Stairs	0.02130427			0.026576175		
VLVM	No Brace Stairs	0.021644224			0.018950318		
VLVM	No Brace Stairs	0.022543478	0.02	0.000640295	0.016813356	0.02	0.005132136
VLVM	Web Stairs	0.379441185			0.722643372		
VLVM	Web Stairs	0.418448921			0.600608575		
VLVM	Web Stairs	0.480239974	0.43	0.050826721	0.583872903	0.64	0.075751587